Comparative Differential Cuproproteomes of Rhodobacter capsulatus Reveal Novel Copper Homeostasis Related Proteins

Journal:	*Metallomics*
Manuscript ID	MT-ART-12-2019-000314.R1
Article Type:	Paper
Date Submitted by the Author:	21-Feb-2020
Complete List of Authors:	Selamoglu, Nur; University of Pennsylvania, Biology Onder, Ozlem; University of Pennsylvania Perelman School of Medicine, Pathology and Laboratory Medicine Ozturk, Yavuz; University of Pennsylvania, Biology Khalfaoui-Hassani, Bahia; University of Pennsylvania, Biology Blaby-Haas, Crysten; Brookhaven National Laboratory, Biology Garcia, Benjamin; University of Pennsylvania Perelman School of Medicine, Department of Biochemistry and Biophysics Koch, Hans-Georg; Albert-Ludwigs-Universität Freiburg, Inst. Biochemie & Molekularbiologie Daldal, Fevzi ; University of Pennsylvania, Biology

SCHOLARONE™
Manuscripts

Significance to Metallomics: (92 words)

The complex response mechanisms of living cells in managing both the deficiency, and the excess, of environmental copper (Cu) continue to intrigue researchers in fields ranging from bacterial pathogens to human diseases. The present paper describes a global label-free quantitative mass spectrometric study of Cu-responsive changes in the proteome of prokaryotic model bacterium *Rhodobacter capsulatus*. 75 proteins, of which ~ 40% were uncharacterized, were strongly influenced (2- to 300-fold) by Cu availability. Probing the function(s)of these proteins using chromosomal deletion mutants demonstrated that several of them are important for cellular Cu homeostasis.

Comparative Differential Cuproproteomes of *Rhodobacter capsulatus* Reveal Novel Copper Homeostasis Related Proteins

Nur Selamoglu[a], Özlem Önder[a,b], Yavuz Öztürk[a,e], Bahia Khalfaoui-Hassani[a,#], Crysten

E. Blaby-Haas[c], Benjamin A. Garcia[d], Hans-Georg Koch[e] and Fevzi Daldal[a*]

[a]Department of Biology, University of Pennsylvania, Philadelphia, PA, 19104 USA;

[b]Department of Pathology and Laboratory Medicine, Perelman School of Medicine,

University of Pennsylvania, Philadelphia, PA 19104, USA; [c]Biology Department,

Brookhaven National Laboratory, Upton, NY 11973, USA; [d]Department of Biochemistry

and Biophysics, Perelman School of Medicine, University of Pennsylvania, Philadelphia,

PA 19104, USA, [e]Institute of Biochemistry and Molecular Biology, ZBMZ, Faculty of

Medicine, Albert-Ludwigs University of Freiburg, 79104 Freiburg, Germany.

Running Title: *Rhodobacter capsulatus* Copper-Responsive Proteome

Key words: *Rhodobacter capsulatus proteome,* differential cuproproteomics, copper

homeostasis, copper-responsive proteins, uncharacterized proteins.

[#]Present address: IPREM, UMR CNRS 5254, and Université de Pau et des Pays de

l'Adour, BP1155 Pau, France.

1

*Corresponding author: Fevzi Daldal

fdaldal@sas.upenn.edu; +1 215-898-4394

Abbreviations

Cu, copper; BCS, bathocuproine sulfonate; Gm^R, gentamicin resistance; MS, mass spectrometry; MS/MS, tandem mass spectrometry; Ps, photosynthetic; Res, respiratory; cbb_3-Cox, cbb_3-type cytochrome c oxidase; MCO/CutO, multicopper oxidase; (+Cu), Cu-excess; (+BCS), Cu-depleted; nLC-MS/MS, nano liquid chromatography/tandem mass spectrometry; ICP-MS, inductively coupled plasma mass spectrometry; GTA, gene transfer agent; LFQ, label-free quantitation; DDA, data-dependent acquisition; HCD, high-energy collision dissociation; AGC, automatic gain control; FDR, false discovery rate; FC, fold change; Cu^S, Cu sensitive; Cu^R, Cu resistant; UniprotKB, Uniprot knowledge base; RND-type, resistance, nodulation, cell division protein family.

ABSTRACT

Copper (Cu) is an essential, but toxic, micronutrient for living organisms and cells have

developed sophisticated response mechanisms towards both the lack and the excess of

Cu in their environments. In this study, we achieved a global view of Cu-responsive

changes in the prokaryotic model organism *Rhodobacter capsulatus* using label-free

quantitative differential proteomics. Semi-aerobically grown cells under heterotrophic

conditions in minimal medium (~ 0.3 μM Cu) were compared with cells supplemented

with either 5 μM Cu or with 5 mM of the Cu-chelator bathocuproine sulfonate. Mass

spectrometry based bottom-up proteomics of unfractionated cell lysates identified 2430

of the 3632 putative proteins encoded by the genome, producing a robust proteome

dataset for *R. capsulatus*. Use of biological and technical replicates for each growth

condition yielded high reproducibility and reliable quantification for 1926 of the

identified proteins. Comparison of cells grown under Cu-excess or Cu-depleted

conditions to those grown under minimal Cu-sufficient conditions revealed that 75

proteins exhibited statistically significant ($p<0.05$) abundance changes, ranging from 2- to

300-fold. A subset of the highly Cu-responsive proteins was orthogonally probed using

molecular genetics, validating that several of them were indeed involved in cellular Cu

homeostasis.

1
2
3
4
5
6
7
8
9
10
11
12
13
14
15
16
17
18
19
20
21
22
23
24
25
26
27
28
29
30
31
32
33
34
35
36
37
38
39
40
41
42
43
44
45
46
47
48
49
50
51
52
53
54
55
56
57
58
59
60

4

INTRODUCTION

The complex response mechanisms of living cells in handling environmental copper (Cu) continue to intrigue researchers in fields ranging from human diseases to bacterial pathogens [1]. Cu is a required micronutrient stringently regulated in eukaryotic and prokaryotic organisms, leading to a variety of lethal disorders when uncontrolled [2, 3]. Understanding its homeostasis is a recognized challenge, but there is a paucity of information about the cuproproteomes of all organisms. Even the list of specific components involved in cellular Cu trafficking and their mechanistic roles is often largely incomplete [4, 5].

The Gram negative, purple non-sulfur phototrophic bacterium *Rhodobacter capsulatus* is frequently used for studying a wide variety of metabolic processes. Its versatile growth abilities extending from anoxygenic photosynthetic (Ps), aerobic respiratory (Res) to autotrophic and heterotrophic growth modes are unparalleled [6]. Ongoing molecular studies, augmented with diverse biochemical, biophysical and structural investigations, continuously shed light onto key cellular processes carried out by *Rhodobacter* species [7-12]. Discoveries of novel components and their mechanisms of function and biogenesis are increasing our knowledge about the physiology of this organism [13, 14]. *R. capsulatus* is also a model organism for analyzing the sophisticated networks of Cu detoxification and cuproprotein assembly pathways for metabolically important cuproenzymes, including

5

the cbb_3-type cytochrome c oxidase (cbb_3-Cox), nitrous oxide reductase and multicopper

oxidase [14-18]. Thus, a comprehensive characterization of its proteome and determination

of its Cu-responsive proteins would be important for these studies. Only a few partial

studies have been conducted in the past [19-23], hence a need for a more complete and

quantitative proteomic database for this species. Our earlier attempt offered a qualitative

glimpse into *R. capsulatus* proteome, focusing on the periplasmic sub-proteome, and

identifying ~ 13% of its predicted proteins [19, 23]. Benefiting from recent advances, we

initiated a new study for a more comprehensive description of *R. capsulatus* proteome.

Moreover, as ~ 20% of *R. capsulatus* genes encode uncharacterized proteins (Uniprot

Knowledge Base, UniprotKB) we also aimed to document the occurrence and plausible

function(s) of these hypothetical proteins, and comparative quantification of key proteins

respondin to the presence or absence of Cu in the environment.

Past studies have defined some key players involved in Cu homeostasis in bacteria,

including the P_{1B}-type Cu ATPase CopA, the transcription regulator CueR, the Cu efflux

transporter CusCFBA, and the multicopper oxidase CueO involved in Cu homeostasis [24-28]. In *R. capsulatus*, the bacterial Cu importer CcoA, the general and specialized P_{1B}-type

Cu export ATPases (CopA and CcoI, respectively), the cytoplasmic (CopZ) and

periplasmic (SenC and PccA) Cu chaperones, as well as a novel cupric reductase (CcoG)

involved in the biogenesis of cbb_3-Cox have been investigated [14, 17, 29-31]. Still, many aspects

of Cu homeostasis remain unknown beyond the cbb_3-Cox dependent respiration in this

species. In particular, the transcriptional and translational regulation of Cu homeostasis, and its possible links to other transition metals are unexplored [32]. We reasoned that mass spectrometry based quantitative proteomics, comparing cells grown in the presence or absence of Cu, may reveal hitherto unknown Cu-responsive proteins involved in Cu homeostasis.

In this study, we identified a total of 2430 *R. capsulatus* proteins, reliably expanding the previously experimentally defined proteome size by about five fold (from 13% to 67%). Moreover, using label-free quantification (LFQ) [33], we established relative abundances for 1926 of the identified proteins in a wild type *R. capsulatus* strain as a result of growth under different Cu amounts. Remarkably, 75 proteins exhibited statistically significant ($p<0.05$) Cu-responsive abundance changes that ranged from 2 to 300-folds. Of these proteins affected by the presence or absence of Cu in the growth environment, 44 corresponded to proteins with previously attributed/predicted functions, whereas 31 remained uncharacterized. Additional molecular genetics and bioinformatics approaches established that several of them indeed impacted Cu homeostasis.

EXPERIMENTAL PROCEDURES

Growth conditions and strains used

All strains and plasmids are listed in **Table S1**, **Supplementary Data**. *R. capsulatus* wild type strain MT1131 (a 'green' derivative of SB1003) [34] was grown chemoheterotropically with succinate as a carbon source, under semi-aerobic conditions at 35 °C. The Sistrom's minimal medium A (MedA) [35] prepared using metal-free water (Millipore) without added $CuSO_4$ was used as liquid or solid growth media. This medium (referred to as Cu-sufficient control, CTRL) contained ~ 0.3 µM Cu, which was fully sufficient to support optimal growth and produce active cbb_3-Cox in cells [36], provided a baseline control. It was supplemented with 5 µM Cu, or with 5 mM of the Cu-chelator bathocuproine-disulfonic acid (BCS) (Sigma, Inc.) to yield Cu-excess (+Cu) or Cu-depleted (+BCS) media, respectively. No growth inhibition occurs using +Cu, and no active cbb_3-Cox is produced in cells grown in +BCS media [37]. Cells were harvested around the mid-exponential growth phase (OD_{630} ~ 0.6 to 0.8), washed with Cu-sufficient medium and stored at - 80°C until use. Three independently grown culture replicates were used for each of the three different growth conditions, yielding a total of nine biological samples. Determination of total cellular metal contents using ICP-MS indicated that Cu-sufficient, +Cu and +BCS cells contained 6.9 (+/- 0.8), 20.2 (+/- 2.9) and 1.1 (+/- 0.5) µg of Cu per g of lyophilized cells, respectively. Mn levels were unchanged under these

conditions, and only marginal variations on the amounts of Fe and Zn were observed (**Figure S5**). The presence or absence of the cbb_3-Cox activity was verified by staining colonies with a mixture (1:1, v/v) of 35 mM α-naphthol in ethanol and 30 mM N,N,N',N'-dimethyl-p-phenylenediamine in water (*i.e.*, "Nadi staining" procedure) [38]. Colonies producing active cbb_3-Cox turned blue within seconds after exposure to this mixture, while those lacking it remained unstained [39] (**Figure S1**).

Sample preparation, protein extraction and digestion

A urea/thiourea lysis/extraction and Lys-C/trypsin digestion method was used as protocol (A): 100 mg wet cell pellets were resuspended in a freshly prepared lysis buffer containing 6 M urea, 2 M thiourea, 50 mM ammonium bicarbonate and HALT™ protease (Thermo Scientific, Inc). Cells were disrupted completely by multiple rounds of sonication on ice, extracts were reduced with 10 mM dithiothreitol (Sigma, Inc.) at room temperature for one hour, and alkylated in the dark with 20 mM iodoacetamide (Sigma, Inc.) at room temperature for 30 min. The reduced and alkylated proteins were first digested with Lys-C (lysyl endopeptidase, WAKO Pure Chemical Industries, Osaka, Japan) for three hours, then diluted 10-fold with 20 mM ammonium bicarbonate (pH 8.5) buffer and further digested overnight at 37 °C with mass spectrometry (MS) grade trypsin (Promega, Inc.) at an enzyme to protein ratio of ~ 1 to 50 (w/w). The tryptic peptides thus generated were acidified with 5 % formic acid to pH ≤ 3, and desalted using Poros Oligo

R3 reverse-phase micro-columns, made of P200 pipet tips pre-plugged with C_{18} disc material (3M Empore, Bioanalytical Technologies) and packed with Poros Oligo R3 matrix (Applied Biosystems, Inc). Purified peptides were lyophilized and stored at - 80 °C until mass spectral analysis. An alternative protocol (B) for extract preparation and digestion with trypsin, in the presence of the ProteaseMAX™ enhancer (Promega Inc.), was also used (**Supplementary Data**). In tests, the urea/thiourea extraction and Lys-C/trypsin digestion protocol (A) yielded ~ 40% more protein identifications than protocol (B) and was opted for all quantitative analyses, while data from both extraction methods were combined for qualitative identifications

ICP-MS analyses

Samples for determination of total cellular Cu contents were prepared as described earlier [17], and total metal content was measured by ICP-MS (Nexion 350D, Perkin Elmer equipped with an Element Scientific prepFAST M5 autosampler), using three biological and three technical repeats for Cu-sufficient, Cu-excess (+Cu) and Cu-depleted (+BCS) conditions [40].

Nano LC-MS/MS analyses

A nano-LC-MS/MS coupled to either a Thermo Q-Exactive or to a Thermo Orbitrap Velos Pro mass spectrometer was used for data collection. For quantitative analyses, only

the data obtained using the higher sensitivity Q-Exactive MS and the more efficient urea/thiourea extraction protocol (A) were opted. However, for defining *R. capsulatus* whole proteome, all protein identifications derived from both protocols A/Q-Exactive and B/Orbitrap Velos were combined. The Orbitrap Velos Pro MS parameters are described in the **Supplemental Data**.

The Q-Exactive Orbitrap MS was coupled to an Easy-nLC™ 1000 nano liquid chromatography system (Thermo Fisher Scientific, San Jose, CA) for analyzing protein digests. Samples were loaded in buffer A (0.1% formic acid) onto an 18 cm fused silica capillary column (75 μm internal diameter), packed in-house with reversed-phase Repro-Sil Pur C18-AQ 3 μm resin (Dr. Maisch GmbH, Germany). Elution was performed with a 120 min linear gradient from 2 to 30 % buffer B (100% acetonitrile, 0.1% formic acid), followed by a 15 min linear gradient from 30 to 90% buffer B, with a constant flow rate of 300 nL/min. At the end of the gradient, the column was washed for an additional 5 min with 90 % buffer B. The Q-Exactive MS was operated (Thermo Xcalibur, version 2.2) in the data-dependent acquisition (DDA) mode with dynamic exclusion enabled (repeat count: 1, exclusion duration: 20 sec). Full MS spectrum scans (m/z 350–1600) were acquired at a resolution of 70,000 (at 200 m/z), and the fifteen most intense ions were selected for MS/MS with high-energy collision dissociation (HCD) at a normalized collision energy of 22 at a resolution of 17,500 (at 200 m/z). Lock mass calibration was implemented using polysiloxane ions 371.10123 m/z and 445.12000 m/z, and the

automatic gain control (AGC) targets of full MS and MS/MS scans were 1×10^6 and 5×10^4, respectively. Unassigned charge states and singly-charged species were rejected.

Search parameters and acceptance criteria: Qualitative data analysis

MaxQuant version 1.5.5.1 (www.coxdocs.org) [41] was used for raw MS data analysis. MS/MS spectra were searched by the Andromeda search engine [42] against the *R. capsulatus* strain SB1003 FASTA database (UniprotKB, 3632 entries; www.uniprot.org; date of last modification 2010) as well as for reverse database and common contaminants, both being defaults within the MaxQuant software. Methionine oxidation and N-terminal acetylation were assigned as variable modifications, and carbamidomethyl-cysteine was used as a fixed modification. Full trypsin digestion (K/R) was specified with two missed cleavages allowed. The minimum peptide length was set to seven amino acids. For matching between runs, the retention time alignment window was set to 20 min, and the match time window to 1 min. The matching option was used only among sample runs for a given LC-MS instrument *(i.e.,* runs analyzed by the Q-Exactive MS were not matched with Orbitrap Velos Pro MS runs). MS/MS fragment mass tolerance was 20 ppm and other search parameters in MaxQuant were set to default values.

For each protein identified, the acceptance criteria included false discovery rate (FDR) = 0.01, minimum number of peptides = 1, and minimum number of MS/MS spectra = 1. Samples prepared using both lysis protocols (A,B) coupled with nLC-MS/MS instruments

1

(*i.e.*, A/Q-Exactive and B/Orbitrap Velos), with all biological and technical replicates were grouped together to generate a highly redundant data set with high reliability for the identified proteins.

Experimental design and statistical rationale: Quantitative data analysis

The experimental design for the quantitative aspect of this study used for each of the three Cu conditions [Cu-excess (+Cu), Cu-depleted (+BCS) and Cu-sufficient control (CTRL)] three independent biological replicates, yielding a total of nine samples. Samples were lysed/digested in parallel using protocol (A) and analyzed by at least three technical replicates on the Q-Exactive. Thus, each Cu growth condition was represented by a minimum of nine nLC-MS/MS runs.

Following MaxQuant analyses, quantitative evaluation was performed using the Perseus platform (version 1.6.0.2, www.coxdocs.org) [33]. The data were processed and filtered according to Perseus defaults, and the LFQ values were converted to log2 scale and normalized by subtraction of means. Only proteins that were detected in at least five sample runs (among nine or more) in at least one or more Cu groups (Control, +Cu, +BCS) were retained, allowing to preserve those proteins that were present under one copper condition but absent in another. These proteins were referred to as "reliably quantifiable" proteins. Missing value imputation was performed by replacing values from the normal distribution (per defaults in Perseus, with 0.3 width and 1.8 downshift). Pearson

correlations among individual experimental runs, including biological and technical

replicates for all three Cu concentrations, were very high (> 0.919-0.992) (**Figure S2**). Only

one technical replicate that exhibited correlation values ranging from 0.752 to 0.841

(green) was not in line with the rest of the data, and discarded. To identify the proteins

that were significantly changed in response to the different Cu concentrations used,

Student's two-sample t-tests were performed for (+Cu) and (+BCS) samples in

comparison with the control (Cu-sufficient) samples. Each Cu concentration was

represented by at least nine (biological and technical triplicates) independent

measurements, which provided reliable statistical power for the t-tests. The proteins with

a p-value < 0.05 and fold-change > 2 for abundance changes were considered as being

"Cu-responsive" to the presence or absence of Cu in the growth medium.

Chromosomal inactivation of selected Cu-responsive genes

    Chromosomal knock-out alleles of selected *R. capsulatus* genes based on their

pronounced Cu-responses were obtained by either the interposon mutagenesis via the

Gene Transfer Agent (GTA) [43], or by an in-frame, marker-less chromosomal deletion

method, adapted from [44]. The GTA mediated chromosomal inactivation was used for the

gene clusters [*rcc00885-rcc00891*], [*rcc01027-rcc01031*] and [*rcc03065-rcc03067*] and for the

single genes *rcc00738, rcc01423, rcc01445 and rcc02109.* The corresponding deletion-

insertion alleles in the conjugative pRK415 plasmid were obtained using the gentamicin

resistance (Gm^R) cassette [45] and the HiFi Gibson assembly method, as described by the manufacturer (NEB Lab, MA) (**Figure S3**). Approximately 80 to 200 base pairs long N-terminal and C-terminal portions of a given gene, flanked by 450 to 600 base pairs at its 5′ and 3′ ends, were amplified by PCR using the wild type MT1131 genomic DNA as a template. The PCR primers contained 20 to 30 base pairs long 5′ overlapping regions between the vector arms and the two gene fragments, and 20 to 24 base pairs long gene-specific sequences, as appropriate (**Table S2**). Separately, the 1.2 kb long Gm^R cassette was PCR amplified using the plasmid pCHB::Gen (**Table S1**) as a template and the Gm-F and Gm-R primers, and the PCR product thus obtained was digested with DpnI in order to remove the template. The quantity and quality of the amplified DNA fragments were checked by using a nanodrop spectrophotometer and agarose gel electrophoresis, respectively, prior to the assembly reactions. HiFi assembly master mix (NEBuilder^R) was used in a single step reaction to assemble together the N-terminal portion of the target gene, the Gm^R cassette, the C-terminal portion of the target gene, and the conjugative plasmid pRK415 [46] that was digested with KpnI and XbaI restriction enzymes (**Figure S3a**), following the manufacturer's protocol. In each case, the total amount of DNA fragments used was ~ 0.4 - 0.5 pmoles, and the vector to insert ratio was ~ 1:2 to 1:3. The samples were incubated in a thermocycler at 50 °C for 60 minutes, and 4 μl of assembly reaction was transformed to chemically competent *E. coli* HB101 strain for Gm^R. The assembled deletion-insertion allele in the conjugative pRK415 plasmid of the target gene

1

was confirmed by restriction enzyme digestion and subsequent DNA sequencing. The correct clones in the broad host range plasmid pRK415 were conjugated into the GTA overproducer *R. capsulatus* Y262 strain [47] via triparental crosses (**Table S1**), and the enriched GTA was used to inactivate the chromosomal copy of the desired genes in wild-type *R. capsulatus* MT1131 strain [43]. The deletion-insertion mutant of *rcc02110*, corresponding to the multicopper oxidase (MCO/CutO) enzyme had been reported earlier [16].

The in-frame, marker-less chromosomal deletion method was used for *R. capsulatus* genes *rcc00098, rcc01423* and *rcc02111.* The mutants contained in-frame deletions of the entire coding sequence of a given gene, except its first four and last four codons. The alleles were constructed by joining the ~ 900 to 1000 base pairs long 5′ flanking region of the target gene and its first four codons with its ~ 900 to 1000 base pairs long 3′ flanking region and its last four codons to the suicide plasmid pZDJ (**Figure S3b**) [44]. The fragments used in the assembly method were PCR amplified using the MT1131 genomic DNA as a template, the specific primers containing 25 base pair 5′ overlapping region between the vector arms and gene fragments (**Table S2**), and the plasmid pZDJ, linearized by the SalI and SacI restriction digestions. Following the qualitative and quantitative controls of the PCR amplified DNA fragments by nanodrop spectrophotometer and by agarose gel electrophoresis, the HiFi assembly master mix (NEBuilder^R) was used as above**,** and 2 μl of the assembly reaction was transformed into chemically competent *E. coli* strain S17-1

(**Table S1**). The assembled in-frame deletion alleles of the target genes were confirmed

by restriction enzyme digestion and DNA sequencing, and the resulting plasmids were

conjugated into the wild type *R. capsulatus* strain MT1131, selecting for Gm^R

transconjugants. The plasmid pZDJ derivatives being unable to replicate in *R. capsulatus*,

the Gm^R transconjugants could only arise via a single crossover between the homologous

5′ or 3′ end of the target gene and its chromosomal counterpart. These clones were tested

for their inability to grow on MedA containing 10% sucrose, which is toxic in the presence

of *sacB* carried by plasmid pZDJ derivatives. Chromosomal deletions were then selected

for their abilities to grow under aerobic conditions in the presence of 10% sucrose, due to

a second recombination event eliminating the chromosome-integrated copy of pZDJ [44, 48].

The resultant sucrose resistant and Gm^S colonies were screened by PCR to detect the

expected size changes due to the desired in-frame deletions, and confirmed by DNA

sequencing using the appropriate primers after PCR amplifications (**Table S2**).

Phenotypic characterization of chromosomal deletion mutants

Mutants carrying the chromosomal deletion alleles obtained either by the interposon

mutagenesis via GTA, or the marker-less in-frame deletion, methods were tested for their

abilities to grow under Res and Ps conditions on enriched MPYE or minimal MedA (Cu-

sufficient CTRL), (+Cu) and (+BCS) media. Growth was scored after two to three days of

incubation at 35 °C, and the mutants that were able to grow under Res conditions were also characterized for their cbb_3-Cox (NADI staining) phenotypes (**Figure S1**).

RESULTS

Proteome of R. capsulatus under respiratory growth conditions

In this study, we sought to establish a comprehensive proteome for *R. capsula*tus (strain MT1131) cells grown heterotrophically in minimal medium (MedA) with succinate as the carbon source. For a qualitative description of the proteome, MS-based identification data from 18 independently prepared samples (3 biological replicates x 3 Cu levels x 2 lysis/MS methods; see Experimental Procedures) subjected to a total of 58 nLC-MS/MS runs were combined into a single dataset with high redundancy and reliability. This dataset contained more than 33,000 independently sequenced peptides obtained using routine nLC-MS/MS conditions without any prefractionation and overall analyses identified 2430 (67%) out of 3632 *R. capsulatus* proteins (UniprotKB) (**Figure 1A**) (**Table S3**, sheets 1, 2 and 3). As a result of high data redundancy, more than 97% of the identified proteins (2371) were characterized by multiple peptides, and only 59 were identified by a single unique peptide, of which only 13 relied on single spectra (**Table S3**, sheet 4: single peptide ID; annotated spectra in **Figure S4**).

The previously available *R. capsulatus* proteomic dataset, obtained using 2D/SDS-PAGE based separations and a limited sensitivity ion trap MS, contained fewer than 500

proteins [19]. The new dataset increased the number of identified proteins by about five-fold, yielding a fairly complete *R. capsulatus* proteome present under the growth conditions used. Moreover, almost half of the 780 putative proteins annotated as "uncharacterized" on the *R. capsulatus* genome (UniprotKB) were also identified (371/780 or 48%), with 353 likely being documented the first time for their occurrence in cells (**Figure 1A**, tan color oval).

For an brief overview of the proteome, all identified proteins were classified based on their predicted cellular localizations and physiological functions using PSORTb (www.psort.org; version 3.0.2;) and TIGR annotation (www.jcvi.org/tigrfams; release 15.0, 2014) platforms, respectively (**Figure 1B** and **C)**. The cytoplasmic (1258) and inner membrane (464) proteins were more frequent than the periplasmic (82), outer membrane (31), and extracellular proteins (15), although a fraction of them (580) remained of unknown location according to PSORTb. Only a portion of the identified proteins could be functionally classified using the primary cellular functions of the TIGR database (**Figure 1C**). The proteins that are involved in protein synthesis (125), energy metabolism (116), cofactor biosynthesis (91), protein fate (76) and transport (70) exhibited a distribution similar to that seen earlier for this organism [19]. Additional complementary annotations associated with the identified proteins in other similar databases (*e.g.*, Gene Ontology, KEGG and Interpro) are included in **Table S3**.

Relative abundance **of** *R. capsulatus proteins under respiratory Cu-sufficient growth conditions*

We assessed the relative abundances of the identified proteins under different growth conditions using their LFQ intensities (Experimental Procedures). The stringent filter imposed (protein identified in at least five out of nine or more repeat measurements for a given Cu level, see Experimental Procedures) indicated that a large fraction (1926/2430 or 79%) of them were reliably quantifiable (**Figure 1A**) (**Table S3,** sheet 5, Quantified-Statistics), and the list included many uncharacterized proteins (257 out of 1926, or 13%). This dataset of 1926 quantifiable proteins was used for subsequent quantitative analyses.

The LFQ intensity-based abundances of *R. capsulatus* proteins under the Cu-sufficient (control) growth conditions was visualized by plotting the mean $\log_2$ LFQ values against the protein rank (**Figure 2**). LFQ values spanned a wide ~ 8000 fold change from the highest to the lowest, and the two extremes are highlighted in the figure insets. The LFQ intensities were not taken as direct reflections of cellular protein abundances as they are affected by multiple factors, including protein size, digestion efficiency, and number and ionization properties of peptides and others. Nevertheless, in this case the highest LFQ proteins corresponded to those that are generally present copiously in cells, and were mostly located in the cytoplasm (**Figure 2**, upper right). They included the translation machinery components such as EF-Tu and EF-G (Rcc00147, Rcc00296), 30S and 50S ribosomal subunits (Rcc01125, Rcc00290) and the ribosome-associated chaperone trigger

factor (Rcc02008), the chaperonin GroL (Rcc02478), and several metabolic enzymes like GA3P dehydrogenase (Rcc02160), malate dehydrogenase (Rcc00718) and isocitrate dehydrogenase (Rcc01887), as well as soluble components of membrane transporters such as the F1 subunits of the ATP synthase (Rcc02971, Rcc02973) and ABC-type and dicarboxylate transporters (Rcc01369, Rcc03024). Although most of the components of the photosynthetic machinery of *R. capsulatus* were not produced, yet a few membrane-integral components corresponding to the B800-850 light-harvesting complex gamma subunit (Rcc02533, *pucD~E* fusion protein) and the photosynthetic reaction center H subunit (Rcc00659) were seen, possibly reflecting the photosynthesis-ready state of cells grown under semi-aerobiosis. The lowest LFQ proteins (**Figure 2**, lower left) included the multicopper oxidase CutO (Rcc02110), the RNA/peptide degradation enzymes M4 family peptidase (Rcp00068) and SsrA binding protein (Rcc03380), and nitrous oxide maturation protein NosD (Rcp00074). Cytoplasmic enzymes such as nucleotidyl-transferase (Rcc00039) and glycosyl-transferase (Rcc02217), and a XRE family member transcription regulator (Rcp00105) were also of low intensity, together with the poorly characterized proteins such as NosL family protein (Rcc00889) and conserved domain protein (Rcc01278) and five other uncharacterized proteins. As expected, some of the low abundance proteins (*e.g.*, MCO/CutO) exhibited strong differential abundance changes in the presence or absence of Cu (see below).

2

Cu-related proteins of R. capsulatus

Among the *R. capsulatus* proteins identified in the present study (**Table S3, sheet 1**), we distinguished those that corresponded to either known members of Cu homeostasis and cuproproteins biogenesis processes [14, 18] or predicted to be so, based on their homologies to Cu-related proteins characterized in other organisms [24, 27] (**Table 1**). The Cu tolerance conferring proteins, such as the components associated with the RND-type Cu efflux pump, CusRS and CusABCF, the P_{1B}-type Cu-ATPase CopA and its chaperone CopZ, and the multicopper oxidase CutO (CueO in *E. coli*) were all detected. Similarly, most of the known *R. capsulatus* cuproproteins and the components involved in their biogenesis were readily recognized: this included components of *cbb₃*-Cox (CcoNOQP) and its assembly proteins-CcoGHIS, CcoA, SenC and PccA [14, 18], the NosRLYFDX for the nitrous oxide reductase NosZ [49], and the putative Cu-responsive transcriptional regulators (CsoR and CueR) that are homologous to their counterparts in other organisms. In addition to the known Cu cofactor containing enzymes such as *cbb₃*-Cox, CutO [50] and NosZ, putative cuproteins like the polyphenol oxidase/tyrosinase (Rcc02805) and pseudoazurin (Rcp00043) that might act as an electron donor to N_2O reductase [51] were also found. Proteins whose corresponding genes were adjacent to known Cu homeostasis proteins, like Rcc02111 and Rcc2109 adjoining MCO/CutO (Rcc002110), and those flanking CopZ (Rcc03125), Rcc03124 and Rcc03126 (similar to

2

Bacillus subtilis YphP, an oxidoreductase with a CXC catalytic motif [52]), were included in

Table 1.

Quantification of changes in R. capsulatus proteins in response to varying Cu concentrations

In order to reliably define the differential abundances among the *R. capsulatus* proteins

in response to different Cu concentrations available to cells, the quality of the LFQ data

was examined using Pearson correlation (**Figure 3A),** where the scatterplots and

correlation heatmap represents biological replicates of cells exposed to differing Cu

concentrations. The reproducibility of the data was excellent, with the correlation factors

above 0.959, despite the changing Cu levels in growth conditions. Moreover, for a given

Cu condition, the correlation among the biological replicates was highest, ranging from

0.978 to 0.994. As expected, the correlation factors corresponding to cells exposed to

differing Cu amounts were slightly lower due to quantitative changes specific to the

changing growth conditions, and the lowest correlation coefficients ranging from 0.959

to 0.974 (**Figure 3A,** nine yellow-orange squares) corresponded to the Cu-excess (+Cu)

versus the Cu-depleted (+BCS) conditions.

Next, an unsupervised principal component analysis (PCA) for the three different

concentrations of Cu used was conducted using the LFQ values of the 1926 quantifiable

proteins to further independently probe the quality of the data. This analysis showed that

the three biological replicates clustered in the proximity of each other, and into three groups corresponding to the three Cu amounts used, with (+Cu) samples being most spread out (**Figure 3B**). The variations of the PCA component 1 and component 2 were 39% and 16%, respectively, with the largest differences being between the (+Cu) and (+BCS) samples. Supported by the robust outcomes of the Pearson correlations and the PCA analyses, we analyzed the *R. capsulatus* proteome changes in response to Cu availability in more detail.

Comparative analysis of R. capsulatus proteins affected by the presence or absence of Cu

Using the quantifiable proteins dataset, proteins that exhibited statistically significant abundance changes when cells were exposed to different amounts of Cu (+Cu or +BCS), as compared to control cells (Ctrl), were determined by two-sample t-tests. The results are depicted as volcano plots in **Figure 4** that visually display both the fold-changes and the associated statistical errors (p-values) for +Cu (**A**) and +BCS (**B**) samples. Strongly enriched or depleted proteins are concentrated in the upper right and left quadrants, respectively, for each Cu condition, emphasizing the large fold-changes accompanied by low p-values. Acceptance values of $p < 0.05$ and fold-change > 2 (indicated by dotted lines) defined 75 distinct proteins (red and blue circles) that exhibited significant differential abundance changes in response to Cu-excess (+Cu) or Cu-depletion (+BCS),

or both, compared to Cu-sufficient (control) cells. These proteins are referred to as Cu-

responsive proteins (**Table 2**), and discussed below.

To corroborate the statistical results, the Cu-responsive differentially abundant

proteins were further probed by unsupervised hierarchical clustering of z-scored LFQ

values (**Figure 5**). Individual samples are shown along the horizontal axis for +BCS (11

repeats), control (10 repeats) and +Cu (9 repeats); the 75 proteins analyzed are indicated

in the dendrogram on the left. The proteins clustered into groups and subgroups, and

relative abundance changes accompanying Cu levels are clearly visible (low and high

relative z-scored abundances are indicated by blue and yellow, respectively). A visual

inspection of the data showed that proteins in clusters 1 and 3 were primarily affected by

Cu-depletion (+BCS) as compared to Cu-sufficient (control) samples, with changes in

opposite directions. While cluster 1 proteins strongly increased with Cu-depletion,

cluster 3 proteins decreased. The members of clusters 1 and 3 did not exhibit drastic

differences between the Cu-sufficient (control) and Cu-excess (+Cu) growth conditions,

indicating that these proteins responded primarily to Cu-depletion, especially when

below a necessary minimum control level. In contrast, cluster 2 proteins were unaffected

by changes from Cu-sufficient (control) to Cu-depleted (+BCS) growth conditions.

However, their relative abundances strongly increased under Cu-excess (+Cu)

conditions, indicating their responses to Cu excess in the growth medium. The results of

the hierarchical cluster analysis supported with the statistical results shown in **Figure 4**

and **Table 2**. Specifically, 10 out of the 11 proteins upregulated with Cu-depletion (**Table 2B)** correspond to cluster 1. Proteins down-regulated with Cu-depletion are represented predominantly in cluster 3, with those with the highest fold-changes being in the bottom subgroup in **Figure 5**. All nine proteins upregulated by Cu-excess **(Table 2A)** appear in cluster 2, in agreement with the statistical analyses of the data. The less strongly affected proteins in **Table 2A and B** mostly appeared in the broad cluster 3. Overall, the results of this unsupervised hierarchical clustering are in line with those obtained using statistics based p-values and fold-changes.

Examination of R. capsulatus proteins differentially affected by the presence or absence of Cu

A closer examination of **Table 2** indicates that functional descriptions (UniprotKB) are available for 44 of the 75 Cu-responsive proteins identified in this work (*e.g.*, multicopper oxidase, NosZ, cytochrome *bd* oxidase or cbb_3-Cox), and several of them (15) were defined solely via their similarities to known families of proteins (*e.g.*, ABC type transporters, NmrA family transcription factors or EAL domain family members), leaving their true physiological roles undetermined. The remaining 16 Cu-responsive proteins remained previously uncharacterized (although might have homologues in other species, **Table 2**), leaving unknown the basis for their Cu-responses.

Cu-excess (+Cu) conditions: Growth in the presence of excess Cu affected only 15 proteins, of which ten increased in abundance by as much as 263 - fold, while five decreased, with respect to the control cells (**Figure 4A** and **Table 2A**). Rcc02110 (MCO/CutO) and Rcc02109 (uncharacterized, initially thought to be a transcriptional regulator CutR [50], whose corresponding genes are localized adjacent to each other, displayed the largest increases, in line with the data showing a protective role of an active MCO against Cu toxicity [50, 53]. Fold-changes for the downregulated proteins were more moderate than for overproduced proteins, with Rcc00722 (a putative lipoprotein) and Rcc02042 (CobL) being the most affected (~ 4-fold). The decline in CobL, the decarboxylating precorrin-6Y C5,15-methyltransferase, involved in vitamin B12 synthesis, possibly illustrates the harmful effect(s) of Cu on this enzyme involved in porphyrin and chlorophyll biosynthesis [54]. Intriguingly, another downregulated protein corresponded to a putative cytoplasmic redox component (Rcc03281, peroxiredoxin), reminiscent of the redox-active nature of Cu, targeting the thiol groups of proteins.

Cu-depleted (+BCS) conditions: Growth in Cu-depleted media affected 65 proteins, 11 of which were upregulated and 54 were downregulated as compared to control cells (**Figure 4B** and **Table 2B**). Remarkably, about one half (31 out of 65) of the proteins affected by Cu-depletion were located in the cytoplasmic membrane, and curiously, 18 of them were chemotaxis-related (*e.g.*, methyl-accepting Mcp and Che) proteins, while several others were putative transporters (including iron-siderophore transporters)

2

(**Table 2B**). The data indicated that Cu shortage affected severely the cellular components involved in motility, and also solute transport associated with the competition between Cu and Fe in cells.

Among the up-regulated proteins, five increased dramatically: Rcc00890 (uncharacterized), Rcc01028 (Fe siderophore transporter), Rcc00889 (NosL family), Rcc03085 (*cydA*, subunit of the *bd*-type quinol oxidase) and Rcc00886 (ATP-binding ABC transporter) (from ~ 300- to 5-fold). Rcc00890, Rcc00889 and Rcc00886 are genetically located adjacent to each other, and why these proteins of currently undefined functions respond so strongly to Cu deficiency is unknown. It is noteworthy that Rcc00890 and Rcc00889 are homologous to the NosL assembly component for the cuproenzyme NosZ, which is strongly down-regulated upon Cu-depletion (**Table 2**). This suggests that either cells try to compensate for Cu shortage by inducing additional assembly components for NosZ, or that the NosL homologues are involved in the biogenesis of a different unknown cuproprotein. Curiously, another protein that was overproduced under Cu shortage corresponded to a periplasmic redox enzyme (Rcc00021, cytochrome *c* peroxidase), possibly substituting functionally an unknown cuproprotein involved in cellular redox homeostasis.

Within the 54 down-regulated proteins, NosZ (Rcp00075, N_2O reductase) exhibited the largest fold decrease (~ 20 fold) together with CcoP (Rcc01160), CcoO (Rcc01158) and Rcc00142 (uncharacterized) (~ 6- to 7-fold). Under Cu deficiency, a decrease in the amount

of the cuproenzyme NosZ and Rcp00073 (*nosF*, Cu ABC transporter subunit, which is an assembly component for NosZ) could be expected, considering that NosZ expression might be enhanced in cells grown under semi-aerobic respiratory conditions [55]. Similarly, while the subunits and the assembly components of the cbb_3-Cox (Rcc01157, Rcc01158, Rcc01160, Rcc01161) decreased by 2- to 7-fold, those of the *bd*-type quinol oxidase (CydA) increased 7-fold. Clearly, under Cu starvation, the *bd*-type quinol oxidase, which is not a cuproenzyme, replaces the cuproenzyme cbb_3-Cox as the major respiratory terminal oxidase. This cellular adaptation to the absence of Cu, suggests that selective expression of these oxidases might be regulated by O_2 and Cu availability.

Intriguingly, a small subset (five) of Cu-responsive proteins, Rcc00533 (uncharacterized), Rcc00722 (putative lipoprotein), Rcc00890 (uncharacterized), Rcc01047 (iron siderophore-cobalamin ABC transporter) and Rcc03029 (uncharacterized), showed small but significant changes in both Cu-excess and Cu-shortage conditions, as compared to Cu-sufficient control cells (**Table 2**, indicated with asterisk). In two of these cases, the changes were in the opposite directions, with Rcc01047 increasing by ~ 5 fold in (+Cu) and decreasing by ~ 2.5 fold in (+BCS), whereas Rcc00890 decreasing by ~ 2 fold in (+Cu) and increasing by ~ 299 fold in (+BCS), containing media. This type of response in opposite directions suggests that these proteins may indeed be Cu regulated, and that their steady-state amounts might be directly linked to Cu availability. In the remaining three cases, the abundance changes were in the same directions in the presence and

2

absence of Cu. While the abundance of Rcc00533 increased, that of Rcc00722 and

Rcc03029 decreased upon growth in the presence of (+Cu) or (+BCS). A response to both

the excess or the absence of Cu suggested that the effects, if not experimental outliers,

may be of broad and indirect nature, possibly affecting oxidative homeostasis and stress

conditions in cells [56, 57].

Comparison of LFQ abundances of Cu-responsive proteins with counterparts in control cells

The different LFQ abundances of the 75 Cu-responsive *R. capsulatus* proteins were

compared to their abundances in Cu-sufficient control cells in figure 6, where LFQ

intensities for these are superimposed onto the (Ctrl) LFQ rank plot from figure 2. Cu-

excess (+Cu) and Cu-depleted (+BCS) growth conditions are indicated by red and blue

circles, respectively, and the locations of these points above or below the curve compared

directly the LFQ levels to those in control cells, displaying their up- or down-regulations.

Many of the proteins showing significant changes (*e.g.*, Rcc00890, Rcc02109 and Rcc02110)

were clustered at the lowest LFQ region (**Figure 6**, right), where many increased in

abundance with Cu-excess, while others increased in abundance with Cu-depletion

conditions. Other proteins that displayed significant abundance shifts in response to

changed growth conditions are found along the full range of protein ranking, located

above or below the black abundance curve of the control cells (**Figure 6**, left to middle

3

sections). This group of proteins included Rcc01158 and Rcc01160 (*ccoO* and *ccoP* subunits of *cbb₃*-Cox), Rcp00075 (*nosZ*, N₂O reductase), Rcc03085 (*cydA*, *bd*-type quinol oxidase subunit), Rcc00142 (uncharacterized) and Rcc01047 (Fe siderophore ABC transporter). Collectively, the data indicated that only a moderate number of the Cu-responsive proteins increased in abundance, while the majority decreased, in response to changing Cu concentrations. Moreover, the increases were large and the decreases were modest, reflecting the importance for cells of a fine-tuned homeostasis, controlling Cu toxicity while supplying the needed Cu for cuproprotein biosynthesis.

A selected subset of proteins with strong differential Cu responses for further investigation

The total number of Cu-responsive proteins found in this work being rather large, more stringent filters were applied (fold change >4 and p< 0.01), which identified 18 proteins showing the strongest effects (**Figure 7**). Six of the 18 proteins had characterized Cu-related functions, including the subunits of the *cbb₃*-Cox (Rcc01157-1160, *ccoNOP*) [14], N₂O reductase (Rcp00075, *nosZ*) [58, 59] and MCO (Rcc02110, *cutO*) [53], as well as cyt *bd* oxidase (Rcc03085, *cydA*) which, although not a copper protein, becomes the major terminal oxidase under Cu shortage. The remaining 12 proteins were experimentally unexplored, especially in respect to Cu homeostasis. A subset of the latter poorly characterized proteins was retained for further genetic studies as representative members

3

of different cellular localizations and types of Cu-responses (**Table 3**). These undefined

proteins included Rcc01445 (putative TonB-dependent receptor), Rcc00098 (TonB-

dependent hemin receptor, HmuR; unknown association with copper) and Rcc02109

(uncharacterized, next to CutO) exhibiting increased abundances in response to +Cu, and

Rcc00890 (uncharacterized) and Rcc01028 (iron-siderophore/cobalamin ABC transporter)

with increased abundances in response to (+BCS) growth conditions (**Figure 7**). Three

other proteins with smaller abundance changes, Rcc00738 (uncharacterized, DUF1989

domain-containing), Rcc01423 (uncharacterized, with a putative metal binding motif),

Rcc03067 (uncharacterized, EfeM homologue, possibly containing Cu cofactors and

involved in ferrous iron uptake) as well as the undetected protein Rcc02111

(uncharacterized, located in the *rcc02109-02111* cluster encompassing MCO) were also

retained (**Table 3**). The function(s) of these proteins in the presence or absence of Cu,

under aerobic and anaerobic growth conditions, and their role(s) on cbb_3-Cox biogenesis

were investigated below.

Probing the physiological roles of selected Cu-responsive proteins

The structural genes of the proteins listed in **Table 3** were targeted for knock out

mutations, and the mutants thus obtained compared with strains lacking the Cu importer

CcoA, the Cu exporter CopA and the MCO/CutO enzyme. In each case, the genetic

organizations of the target genes were taken into account to generate the desired

3

chromosomal deletions that completely eliminated the targeted protein(s). Depending on the predicted transcriptional unit(s), the deletion alleles covered either the entire length of a putative gene cluster including the target gene and its surroundings ([*rcc00094-00098*] for *rcc00098*, [*rcc00885-00890*] for *rcc00890*, [*rcc01027-1031*] for *rcc01028* and [*rcc03065-03067*] for *rcc03067*), or were confined to a single gene (*rr00738*, *rrc01445*, *rrc02109*, *rrc01047* and *rrc01423*), as appropriate (Experimental Procedures). This way, any plausible transcriptional or translational downstream effect(s) of the genetic modifications was avoided so that direct correlation(s) between the observed phenotype(s) and the absence of the desired protein(s) in the mutants was possible. The Cu-sensitive (Cu^S) and Cu-resistant (Cu^R) growth phenotypes of the mutants were scored under both aerobic (Res) and anaerobic (Ps) growth conditions, and compared with appropriate *R. capsulatus* strains (**Table 3**).

The Δ[*rcc00094-00098*] and Δ[*rrc00885-00891*] mutants were similar to a wild type strain, being proficient for growth under both the Ps and Res growth conditions, and had no Cu sensitivity or *cbb$_3$*-Cox defect. This suggested that these proteins were either functionally redundant with other(s) performing similar functions, or that their putative function(s) were not essential under the growth conditions tested. Slight growth inhibition was observed in the presence of BCS under the Res growth conditions with the Δ*rcc00738*, Δ*rcc01445* and Δ[*rcc01027-1031*] mutants (**Table 3**). Phenotypes of these mutants were weak and variable, and growth seemed affected by the presence of BCS,

3

which might interfere with other metals and the redox state of the medium while chelating Cu. The Δ[*rcc03065-03067*] mutant exhibited poor growth only under the Res, but not the Ps, conditions in both the +Cu and +BCS media, as well as in the Cu-sufficient control medium. Interestingly, although the genetic data did not show a clear phenotype, the related proteomic data showed significant changes in the levels of these proteins. Lastly, the deletion of the *rrc01423* gene that was initially retained due to its apparent homology to the cytoplasmic Cu chaperone CopZ, with a CxxC metal binding motif and its small size showed only a slight growth inhibition in the presence of Cu or BCS, and a slightly slower Nadi phenotype (**Table 3**).

   The most informative Cu related phenotypes were observed with the *Δrcc02109* and *Δrcc02111* mutants. These mutants were sensitive to Cu under anoxygenic Ps, but not under oxygenic Res growth, and also had slight respiratory growth impairment in the presence of BCS, resembling a mutant lacking the multicopper oxidase CutO (*Δrcc02110*) [53]. The *Δrcc02109* and *Δrcc02111* mutants produced an active cbb_3-Cox (*i.e.*, Nadi$^+$) similar to CutO or CopA. However, they were distinct from a mutant lacking CopA, which is more sensitive to Cu under the Res, rather than the Ps, growth conditions, and unaffected by the presence of BCS (**Table 3**). Remarkably, the degrees of Cu sensitivity of the *Δrcc02109* and *Δrcc02111* mutants under Ps growth were different. The *Δrcc02111* mutant was impaired for growth in the regular Sistrom's MedA containing 1.3 μM Cu, as was the *Δrcc02110* mutant, although they both could grow in Cu-sufficient (~ 0.3 μM Cu) media

(not shown in **Table 3**). Addition of 5 μM Cu (*i.e.*, +Cu medium) halted the Ps growth of

these mutants, which could be restored upon further addition of ~ 2 mM BCS. In contrast,

the *Δrcc02109* mutant was not impaired for growth in regular MedA containing 1.3 μM

Cu or in Cu-sufficient (~ 0.3 μM Cu) media. However, it was sensitive to the presence of

added 5 μM Cu (5.3 μM Cu) (**Table 3**), and again, its Ps growth could be restored upon

addition of ~ 2 mM BCS. Thus, although the absence of either Rcc02111 or Rcc02109

rendered *R. capsulatus* cells Cu-sensitive under anoxygenic conditions, the *Δrcc02111*

mutant was more sensitive (similar to a CutO-minus mutant), whereas the *Δrcc02109*

mutant could tolerate ~ 1 to 2 μM Cu under the Ps growth conditions. Clearly, the data

showed that both the *Δrcc02109* and *Δrcc02111* mutants were Cu-responsive, supporting

the expectation that their products were important for Cu homeostasis. In summary,

overall findings provided a rich source of information about cellular Cu homeostasis and

identified multiple proteins of unknown function for further studies.

DISCUSSION

An aim of this work was to provide a comprehensive and robust proteome dataset for *R. capsulatus* species grown under the Res conditions in minimal medium with succinate as a carbon source. Towards this goal, two different sample preparation methods were coupled with the usage of high performance MS instruments to generate an excellent coverage of the proteins encoded by the genome of this species. A perusal of the genome suggested that roughly 400 of the gene products that were not detected were involved in specific biological processes, such as anoxygenic photosynthesis, nitrogen/carbon fixation, metabolism of specific compounds or induction of lysogenic prophages. Assuming that these proteins were not produced under our growth conditions [6] (**Table S3**, sheet 3, unidentified proteins), this raises the overall coverage to ~ 75% of *R. capsulatus* genome. This proteome coverage is five times larger than that existing previously [19], and provides a useful platform onto which other proteomic variations that occur under desired growth conditions might be integrated in future studies. Especially, the extensions of this dataset to cells grown under Ps or Res conditions with different carbon sources might be highly valuable for studies addressing light dependent energy conversion and their ramifications including H_2 production, N_2 or CO_2 fixation processes [6].

The current study identified ~ 30 Cu-containing or Cu handling-related *R. capsulatus* proteins that were either known, or predicted by homology, to be involved in Cu homeostasis and cuproprotein biogenesis (**Table 1** and **Figure 8**, circles). However, various other proteins known to be involved in Cu homeostasis or Cu tolerance in other bacterial species are not present in *R. capsulatus*. These include the plasmid-encoded Pco (PcoABCD) system of *E. coli* [60] and their homologues in other species, such as YcnJ in *B. subtilis* [61], PcoCD in methanogens [62], CtpI in *Corynebacterium glutamicum* [63], the periplasmic CopI chaperone in *Rubrivivax gelatinosus* [64], the bacterial metallothionein [65], the Cu-Zn superoxide dismutase (Cu-Zn SOD) chaperone CueP in *Salmonella enterica sv typhimurium* [66], the copper amine oxidase in *E. coli* [67], and the Cu storage proteins [68]. Such variations among species illustrate that bacteria have evolved to harbor specific sets of Cu homeostasis proteins and pathways depending on their lifestyles and ecological habitats [69]. Interestingly, a large number of the identified Cu-containing or -related proteins (**Table 1**) were located in the cytoplasmic membrane and periplasm, with a few exceptions being in the outer membrane and the cytoplasm, possibly due to high toxicity of Cu.

A second aim of this work was to quantitatively compare the *R. capsulatus* proteome in response to the presence (+Cu) or absence (+BCS) of Cu in the growth media. Use of label free quantification methodology coupled with multiple biological and technical repetitions resulted in substantially robust statistical data. Comparisons of the proteomes

of cells grown under the (+Cu) or (+BCS) conditions with those grown under Cu-sufficient controls unveiled 75 Cu-responsive proteins exhibiting 2- to 300-fold abundance changes (p< 0.05). Remarkably, low concentrations of additional copper (5 µM), which has no effect on growth, instigated very strong responses in some cases like Rcc02110 (CutO) and Rcc02109 (uncharacterized, next to CutO [70]) (~ 263- and 58-fold, respectively), which were barely detectable in control (0.3 µM Cu) cells. Analogously, depletion of Cu from the growth media led to extreme overproduction of Rcc00890 (uncharacterized), Rcc01028 (Fe siderophore ABC transporter), Rcc00889 (NosL family) (299- , 24- and 10-fold, respectively). While some of the Cu-related proteins were the subunits or assembly factors of known cuproenzymes (*e.g.*, *cbb*$_3$-Cox subunits CcoNOQP and assembly factors CcoGHIS), others were as yet undefined candidates that might be involved in Cu homeostasis. We note that the protein abundance changes monitored in this study reflect the cumulative levels (*i.e.*, steady-state turnover rates) of the proteins in actively growing cells that are adapted to their environments. This is distinct from monitoring immediate transcriptional activation or repression responses of genes upon Cu availability.

Many of the Cu-related and Cu-responsive *R. capsulatus* proteins identified in this work (**Table 1 and 2**) are depicted in **Figure 8,** where shades of red/yellow and blue indicate the fold-changes in abundance of proteins under Cu-excess and Cu-deficient growth conditions, respectively. Proteins that were overproduced or depleted in

3

response to changes in Cu levels are indicated by up or down arrows, respectively, and darker shades reflected higher fold-changes. For example, the nature of the respiratory terminal oxidase in *R. capsulatus* was changed in response to Cu shortage (*i.e.*, + BCS), and cells replaced their Cu containing cyt *cbb*$_3$-Cox (CcoNOQP) with a non-cupric counterpart, *bd*-type cyt oxidase (Rcc03085, CydA) [39]. Similar adaptive examples are common to all organisms, and the replacement of Cu containing plastocyanin with Fe-containing cytochrome as a photosynthetic electron carrier under Cu limitation is well known in *algae* [71]. In contrast, no differential changes were observed with the Cus efflux system proteins, suggesting that addition of 5 μM Cu was insufficient to affect their regulation in *R. capsulatus*.

A salient feature that emerges from this study is the large number of Cu-responsive proteins that were previously unknown to be affected by changing Cu availability. Among the most strongly Cu-responsive proteins (p<0.01 and >4-fold change), four were uncharacterized (UniprotKB), and eight were poorly defined, leaving unknown their specific functions, especially with respect to cellular Cu. The growth phenotypes of the corresponding knockout mutants in response to Cu availability and *cbb*$_3$-Cox production demonstrated that a number of them (*e.g.*, *Δrcc02109* and *Δrcc02110*) were indeed important for maintaining Cu homeostasis in *R. capsulatus*. The mutant (*Δrcc02111)* was highly sensitive to Cu, showing that its uncharacterized product Rcc02111 has an important role against Cu toxicity, although it was undetected under our conditions.

Thus, other Cu-responsive proteins similar to Rcc02111 might exist in addition to the 75

Cu-responsive proteins identified in *R. capsulatus*.

Conversely, other mutants (*e.g.*, *Δ[rcc00094-00098]*, *Δrcc01445*, *Δrcc01423* and

Δ[rcc03065-03067]) had weak or no readily detectable Cu-related or growth phenotypes

despite the strong differential abundance changes seen in response to Cu, suggesting that

they might be accessory or redundant, rather than essential, for Cu homeostasis.

Interestingly, a few iron homeostasis associated proteins, such as the outer membrane

Ton-B dependent receptors Rcc00098 (*hmuR*), Rcc01445, and the periplasmic iron

siderophore/cobalamin ABC transporter Rcc01047, were overproduced with excess Cu,

as previously seen with E. coli in response to Zn excess [32]. *hmuR* is associated with heme

transport, while *rcc01445* and *rcc01047* are identified as ferric siderophore uptake genes,

and *rcc03067* as *EfeM* and part of the *EfeUOBM* ferrous iron uptake system [13]. Future

studies may clarify the role(s) played by iron homeostasis proteins in Cu homeostasis.

A close examination of Rcc01423, which resembled CopZ, indicated that it contained

two additional Cys residues in two regions that were absent in the CopZ family proteins.

Moreover, Rcc01423 was highly homologous to the *Rhodocyclus tenuis* high-potential iron-

sulfur protein (HiPIP) for which a three dimensional structure (1ISU) is available [72]. These

findings suggested that Rcc01423 might be a high potential iron-sulfur protein (HiPIP)-

type [4Fe-4S] cluster bearing cytoplasmic protein, possibly acting as an electron carrier

and interacting with Cu and. The basis of the weak phenotypes associated with the

4

absence of Rcc01423 remains unclear but its pronounced similarity to HiPIP suggests that its Cu-responsive behavior may be a reflection of cytoplasmic competition between Cu and Fe.

In the case of the *[rcc02109-rcc02110-rcc02111]* (*cutR-cutO-Orf635*) cluster, which confers resistance to Cu by increased transcription of *cutO* and *rcco2109* (uncharacterized, although earlier called *cutR* and thought to be a transcription factor) in response to Cu [50, 53], the proteomic data showed dramatic increases in the abundances of multicopper oxidase Rcc02110 (CutO) and Rcc02109 under excess copper conditions. Remarkably, the transcriptional regulation of *rcc02111 (Orf635)*, which was not detected in this study, was reported to be unresponsive to Cu [53]. However, the mutant lacking it (*Δrcc02111)* displayed a pronounced Cu sensitive phenotype, demonstrating that the product of this gene plays an important role against Cu toxicity. While the molecular basis of Cu sensitivity might be rationalized in the absence of CutO (Δ*rcc02110*), which is thought to convert the more toxic Cu^{+1} to less toxic Cu^{2+} in the presence of O_2 [70], the role(s) of Rcc02109 and Rcc02111 in conferring Cu resistance deserves further studies.

In bacterial genomes, functionally related genes often cluster together to respond coordinately to specific environmental changes [73]. Thus, the identification of a Cu-responsive protein may provide additional clues in respect to other proteins encoded by the genes surrounding that of this protein. Indeed, the *[rcc02109-02110-02111]* cluster surrounding CutO provides a good example. The Rcc02109 (uncharacterized) binds ~1.5

Cu atoms per molecule, and is highly homologous to CopG, which is a Cu tolerance conferring protein found in *Vibrio cholerae (VC2216)* [74] and *Cupriavidus metallidurans* [75, 76]. No homolog of *R. capsulatus* Rcc02109/CopG exists in *E. coli* or *Rhodobacter sphaeroides*, and the different regulations as well as degrees of Cu^S phenotypes of mutants lacking Rcc02109 and Rcc02111 suggest that the two proteins might have different role(s) in Cu-homeostasis. Likewise, the role(s) of Rcc03124 (uncharacterized) and Rcc03126 (uncharacterized but similar to *Bacillus subtilis* YphP [52]), which are the products of the genes surrounding *rcc03125* (CopZ) [77], on Cu homeostasis deserve further investigations. Although these proteins were also not found to be Cu-responsive under our conditions, genetic studies might reveal copper sensitivity similar to that seen with *rcc02111*.

In summary, overall information obtained in this study provides an invaluable proteome dataset for *R. capsulatus*, and in particular, it defines a list of Cu-containing or Cu homeostasis related proteins, as well as a set of Cu-responsive proteins identified by monitoring their differential abundance changes upon exposure of cells to different Cu amounts. While the role(s) of some of these proteins are emerging, future characterizations of selected candidate proteins will better define their role in Cu homeostasis and cuproprotein biogenesis in *R. capsulatus*.

4

Acknowledgements

Data Availability

The raw mass spectrometry proteomics data have been deposited to the publicly accessible ProteomeXchange via the PRIDE repository (http://www.ebi.ac.uk/pride/archive/) with the dataset identifier PXD016079.

Conflict of Interest

The authors declare that they have no financial and non-financial competing interests that might be perceived to influence the results and/or discussion reported in this paper.

Author Contributions

All authors have given approval to the final version of the manuscript. NS, OO, BK-H, CEB-H, BAG, H-GK and FD designed and performed all growth and MS experiments, analyzed data and wrote the manuscript. YO performed all molecular genetics experiments, analyzed the constructs and edited the manuscript. BAG provided access to and support for all MS equipment and approaches, CEB-H did the ICP-MS analyses, and FD and NS managed and supervised the study.

References

1. L. J. Stewart, D. Thaqi, B. Kobe, A. G. McEwan, K. J. Waldron and K. Y. Djoko, Handling of nutrient copper in the bacterial envelope, *Metallomics*, 2019, **11**, 50-63.
2. I. Bertini, G. Cavallaro and K. S. McGreevy, Cellular copper management-a draft user's guide, *Coordination Chemistry Reviews*, 2010, **254**, 506-524.
3. H. Pierson, H. Yang and S. Lutsenko, Copper Transport and Disease: What Can We Learn from Organoids?, *Annu Rev Nutr*, 2019, **39**, 75-94.
4. J. J. Braymer and D. P. Giedroc, Recent developments in copper and zinc homeostasis in bacterial pathogens, *Curr Opin Chem Biol*, 2014, **19**, 59-66.
5. H. Ohrvik, J. Aaseth and N. Horn, Orchestration of dynamic copper navigation - new and missing pieces, *Metallomics*, 2017, **9**, 1204-1229.
6. C. N. Hunter, F. Daldal, M. C. Thurnauer and J. T. Beatty, *The purple phototrophic bacteria*, Springer, 2009.
7. J. E. Kumka, H. Schindel, M. Fang, S. Zappa and C. E. Bauer, Transcriptomic analysis of aerobic respiratory and anaerobic photosynthetic states in *Rhodobacter capsulatus* and their modulation by global redox regulators RegA, FnrL and CrtJ, *Microb Genom*, 2017, **3**, e000125.
8. L. Pena-Castillo, R. G. Mercer, A. Gurinovich, S. J. Callister, A. T. Wright, A. B. Westbye, J. T. Beatty and A. S. Lang, Gene co-expression network analysis in *Rhodobacter capsulatus* and application to comparative expression analysis of *Rhodobacter sphaeroides*, *BMC Genomics*, 2014, **15**, 730.
9. A. S. Lang, A. B. Westbye and J. T. Beatty, The Distribution, Evolution, and Roles of Gene Transfer Agents in Prokaryotic Genetic Exchange, *Annu Rev Virol*, 2017, **4**, 87-104.

10.   R. A. Niederman, Development and dynamics of the photosynthetic apparatus in purple phototrophic bacteria, *Biochim Biophys Acta*, 2016, **1857**, 232-246.

11.   A. F. Verissimo and F. Daldal, Cytochrome *c* biogenesis System I: an intricate process catalyzed by a maturase supercomplex?, *Biochim Biophys Acta*, 2014, **1837**, 989-998.

12.   W. R. Hess, B. A. Berghoff, A. Wilde, C. Steglich and G. Klug, Riboregulators and the role of Hfq in photosynthetic bacteria, *RNA Biol*, 2014, **11**, 413-426.

13.   S. Zappa and C. E. Bauer, Iron homeostasis in the *Rhodobacter* genus, *Adv Bot Res*, 2013, **66**, 1-36.

14.   S. Ekici, G. Pawlik, E. Lohmeyer, H. G. Koch and F. Daldal, Biogenesis of *cbb₃*-type cytochrome *c* oxidase in *Rhodobacter capsulatus*, *Biochim Biophys Acta*, 2012, **1817**, 898-910.

15.   B. Khalfaoui-Hassani, H. Wu, C. E. Blaby-Haas, Y. Zhang, F. Sandri, A. F. Verissimo, H. G. Koch and F. Daldal, Widespread Distribution and Functional Specificity of the Copper Importer CcoA: Distinct Cu Uptake Routes for Bacterial Cytochrome *c* Oxidases, *MBio*, 2018, **9**, e00065-00018.

16.   S. Ekici, H. Yang, H. G. Koch and F. Daldal, Novel transporter required for biogenesis of *cbb₃*-type cytochrome *c* oxidase in *Rhodobacter capsulatus*, *MBio*, 2012, **3**, e00293-00211.

17.   S. Ekici, S. Turkarslan, G. Pawlik, A. Dancis, N. S. Baliga, H. G. Koch and F. Daldal, Intracytoplasmic copper homeostasis controls cytochrome *c* oxidase production, *MBio*, 2014, **5**, e01055-01013.

18.   B. Khalfaoui-Hassani, A. F. Verissimo, H. G. Koch and F. Daldal, Uncovering the Transmembrane Metal Binding Site of the Novel Bacterial Major Facilitator Superfamily-Type Copper Importer CcoA, *MBio*, 2016, **7**, e01981-01915.

19.   O. Onder, S. Aygun-Sunar, N. Selamoglu and F. Daldal, A glimpse into the proteome of phototrophic bacterium *Rhodobacter capsulatus*, *Adv Exp Med Biol*, 2010, **675**, 179-209.

20.   M. C. Hoffmann, E. Wagner, S. Langklotz, Y. Pfander, S. Hott, J. E. Bandow and B. Masepohl, Proteome Profiling of the *Rhodobacter capsulatus* Molybdenum Response Reveals a Role of IscN in Nitrogen Fixation by Fe-Nitrogenase, *J Bacteriol*, 2015, **198**, 633-643.

21.   V. Perez, M. Hengst, L. Kurte, C. Dorador, W. H. Jeffrey, R. Wattiez, V. Molina and S. Matallana-Surget, Bacterial Survival under Extreme UV Radiation: A Comparative Proteomics Study of *Rhodobacter sp.*, Isolated from High Altitude Wetlands in Chile, *Front Microbiol*, 2017, **8**, 1173.

22.   K. Woronowicz, J. W. Harrold, J. M. Kay and R. A. Niederman, Structural and functional proteomics of intracytoplasmic membrane assembly in *Rhodobacter sphaeroides*, *J Mol Microbiol Biotechnol*, 2013, **23**, 48-62.

4

23. O. Onder, S. Turkarslan, D. Sun and F. Daldal, Overproduction or absence of the periplasmic protease DegP severely compromises bacterial growth in the absence of the dithiol: disulfide oxidoreductase DsbA, *Mol Cell Proteomics*, 2008, **7**, 875-890.

24. J. M. Arguello, D. Raimunda and T. Padilla-Benavides, Mechanisms of copper homeostasis in bacteria, *Front Cell Infect Microbiol*, 2013, **3**, 73.

25. P. Chandrangsu, C. Rensing and J. D. Helmann, Metal homeostasis and resistance in bacteria, *Nat Rev Microbiol*, 2017, **15**, 338-350.

26. J. Quintana, L. Novoa-Aponte and J. M. Arguello, Copper homeostasis networks in the bacterium *Pseudomonas aeruginosa*, *J Biol Chem*, 2017, **292**, 15691-15704.

27. C. Rensing and S. Franke, Copper Homeostasis in *Escherichia coli* and Other *Enterobacteriaceae*, *EcoSal Plus*, 2007, **2**.

28. C. Rensing and S. F. McDevitt, The copper metallome in prokaryotic cells, *Met Ions Life Sci*, 2013, **12**, 417-450.

29. E. Lohmeyer, S. Schroder, G. Pawlik, P. I. Trasnea, A. Peters, F. Daldal and H. G. Koch, The ScoI homologue SenC is a copper binding protein that interacts directly with the cbb_3-type cytochrome oxidase in *Rhodobacter capsulatus*, *Biochim Biophys Acta*, 2012, **1817**, 2005-2015.

30. P. I. Trasnea, A. Andrei, D. Marckmann, M. Utz, B. Khalfaoui-Hassani, N. Selamoglu, F. Daldal and H. G. Koch, A Copper Relay System Involving Two Periplasmic Chaperones Drives cbb_3-Type Cytochrome *c* Oxidase Biogenesis in *Rhodobacter capsulatus*, *ACS Chem Biol*, 2018, **13**, 1388-1397.

31. D. Marckmann, P. I. Trasnea, J. Schimpf, C. Winterstein, A. Andrei, S. Schmollinger, C. E. Blaby-Haas, T. Friedrich, F. Daldal and H. G. Koch, The cbb_3-type cytochrome oxidase assembly factor CcoG is a widely distributed cupric reductase, *Proc Natl Acad Sci U S A*, 2019, **116**, 21166-21175.

32. Z. Xu, P. Wang, H. Wang, Z. H. Yu, H. Y. Au-Yeung, T. Hirayama, H. Sun and A. Yan, Zinc excess increases cellular demand for iron and decreases tolerance to copper in Escherichia coli, *J Biol Chem*, 2019, DOI: 10.1074/jbc.RA119.010023.

33. J. Cox, M. Y. Hein, C. A. Luber, I. Paron, N. Nagaraj and M. Mann, Accurate proteome-wide label-free quantification by delayed normalization and maximal peptide ratio extraction, termed MaxLFQ, *Mol Cell Proteomics*, 2014, **13**, 2513-2526.

34. P. A. Scolnik, M. A. Walker and B. L. Marrs, Biosynthesis of carotenoids derived from neurosporene in *Rhodopseudomonas capsulata*, *J Biol Chem*, 1980, **255**, 2427-2432.

35. W. R. Sistrom, A requirement for sodium in the growth of *Rhodopseudomonas spheroides*, *J Gen Microbiol*, 1960, **22**, 778-785.

36. H. G. Koch, C. Winterstein, A. S. Saribas, J. O. Alben and F. Daldal, Roles of the *ccoGHIS* gene products in the biogenesis of the cbb_3-type cytochrome *c* oxidase, *J Mol Biol*, 2000, **297**, 49-65.

37. O. Onder, A. F. Verissimo, B. Khalfaoui-Hassani, A. Peters, H. G. Koch and F. Daldal, Absence of Thiol-Disulfide Oxidoreductase DsbA Impairs cbb_3-Type Cytochrome *c* Oxidase Biogenesis in *Rhodobacter capsulatus*, *Front Microbiol*, 2017, **8**, 2576.

38. B. Marrs, C. L. Stahl, S. Lien and H. Gest, Biochemical physiology of a respiration-deficient mutant of the photosynthetic bacterium *Rhodopseudomonas capsulata*, *Proc Natl Acad Sci U S A*, 1972, **69**, 916-920.

39. F. Daldal, S. Mandaci, C. Winterstein, H. Myllykallio, K. Duyck and D. Zannoni, Mobile cytochrome c_2 and membrane-anchored cytochrome c_y are both efficient electron donors to the cbb_3- and aa_3-type cytochrome *c* oxidases during respiratory growth of *Rhodobacter sphaeroides*, *J Bacteriol*, 2001, **183**, 2013-2024.

40. Y. Zhang, C. E. Blaby-Haas, S. Steimle, A. F. Verissimo, V. A. Garcia-Angulo, H. G. Koch, F. Daldal and B. Khalfaoui-Hassani, Cu Transport by the Extended Family of CcoA-like Transporters (CalT) in Proteobacteria, *Sci Rep*, 2019, **9**, 1208.

41. J. Cox and M. Mann, MaxQuant enables high peptide identification rates, individualized p.p.b.-range mass accuracies and proteome-wide protein quantification, *Nat Biotechnol*, 2008, **26**, 1367-1372.

42. J. Cox, N. Neuhauser, A. Michalski, R. A. Scheltema, J. V. Olsen and M. Mann, Andromeda: a peptide search engine integrated into the MaxQuant environment, *J Proteome Res*, 2011, **10**, 1794-1805.

43. F. Daldal, S. Cheng, J. Applebaum, E. Davidson and R. C. Prince, Cytochrome c_2 is not essential for photosynthetic growth of *Rhodopseudomonas capsulata*, *Proc Natl Acad Sci U S A*, 1986, **83**, 2012-2016.

44. C. A. Brimacombe, A. Stevens, D. Jun, R. Mercer, A. S. Lang and J. T. Beatty, Quorum-sensing regulation of a capsular polysaccharide receptor for the *Rhodobacter capsulatus* gene transfer agent (RcGTA), *Mol Microbiol*, 2013, **87**, 802-817.

45. P. Prentki and H. M. Krisch, In vitro insertional mutagenesis with a selectable DNA fragment, *Gene*, 1984, **29**, 303-313.

46. N. T. Keen, S. Tamaki, D. Kobayashi and D. Trollinger, Improved broad-host-range plasmids for DNA cloning in gram-negative bacteria, *Gene*, 1988, **70**, 191-197.

47. H. C. Yen, N. T. Hu and B. L. Marrs, Characterization of the gene transfer agent made by an overproducer mutant of *Rhodopseudomonas capsulata*, *J Mol Biol*, 1979, **131**, 157-168.

48. K. S. Kuchinski, C. A. Brimacombe, A. B. Westbye, H. Ding and J. T. Beatty, The SOS Response Master Regulator LexA Regulates the Gene Transfer Agent of

4

Rhodobacter capsulatus and Represses Transcription of the Signal Transduction Protein CckA, *J Bacteriol*, 2016, **198**, 1137-1148.

49. D. J. Richardson, L. C. Bell, A. G. McEwan, J. B. Jackson and S. J. Ferguson, Cytochrome c_2 is essential for electron transfer to nitrous oxide reductase from physiological substrates in *Rhodobacter capsulatus* and can act as an electron donor to the reductase *in vitro*. Correlation with photoinhibition studies, *Eur J Biochem*, 1991, **199**, 677-683.

50. J. Wiethaus, G. F. Wildner and B. Masepohl, The multicopper oxidase CutO confers copper tolerance to *Rhodobacter capsulatus*, *FEMS Microbiol Lett*, 2006, **256**, 67-74.

51. K. Mattila and T. Haltia, How does nitrous oxide reductase interact with its electron donors?--A docking study, *Proteins*, 2005, **59**, 708-722.

52. U. Derewenda, T. Boczek, K. L. Gorres, M. Yu, L. W. Hung, D. Cooper, A. Joachimiak, R. T. Raines and Z. S. Derewenda, Structure and function of *Bacillus subtilis* YphP, a prokaryotic disulfide isomerase with a CXC catalytic motif, *Biochemistry*, 2009, **48**, 8664-8671.

53. C. Rademacher, R. Moser, J. W. Lackmann, B. Klinkert, F. Narberhaus and B. Masepohl, Transcriptional and posttranscriptional events control copper-responsive expression of a *Rhodobacter capsulatus* multicopper oxidase, *J Bacteriol*, 2012, **194**, 1849-1859.

54. A. Azzouzi, A. S. Steunou, A. Durand, B. Khalfaoui-Hassani, M. L. Bourbon, C. Astier, D. W. Bollivar and S. Ouchane, Coproporphyrin III excretion identifies the anaerobic coproporphyrinogen III oxidase HemN as a copper target in the Cu(+)-ATPase mutant copA(-) of *Rubrivivax gelatinosus*, *Mol Microbiol*, 2013, **88**, 339-351.

55. D. Nellen-Anthamatten, P. Rossi, O. Preisig, I. Kullik, M. Babst, H. M. Fischer and H. Hennecke, *Bradyrhizobium japonicum* FixK2, a crucial distributor in the FixLJ-dependent regulatory cascade for control of genes inducible by low oxygen levels, *J Bacteriol*, 1998, **180**, 5251-5255.

56. M. Solioz, H. K. Abicht, M. Mermod and S. Mancini, Response of gram-positive bacteria to copper stress, *J Biol Inorg Chem*, 2010, **15**, 3-14.

57. A. Barwinska-Sendra and K. J. Waldron, The Role of Intermetal Competition and Mis-Metalation in Metal Toxicity, *Adv Microb Physiol*, 2017, **70**, 315-379.

58. T. Hino, Y. Matsumoto, S. Nagano, H. Sugimoto, Y. Fukumori, T. Murata, S. Iwata and Y. Shiro, Structural basis of biological N_2O generation by bacterial nitric oxide reductase, *Science*, 2010, **330**, 1666-1670.

59. W. G. Zumft, A. Dreusch, S. Lochelt, H. Cuypers, B. Friedrich and B. Schneider, Derived amino acid sequences of the nosZ gene (respiratory N_2O reductase) from *Alcaligenes eutrophus*, *Pseudomonas aeruginosa* and *Pseudomonas stutzeri* reveal

potential copper-binding residues. Implications for the Cu_A site of N_2O reductase and cytochrome-c oxidase, *Eur J Biochem*, 1992, **208**, 31-40.

60. C. Rensing and G. Grass, *Escherichia coli* mechanisms of copper homeostasis in a changing environment, *FEMS Microbiol Rev*, 2003, **27**, 197-213.

61. S. Chillappagari, M. Miethke, H. Trip, O. P. Kuipers and M. A. Marahiel, Copper acquisition is mediated by YcnJ and regulated by YcnK and CsoR in *Bacillus subtilis*, *J Bacteriol*, 2009, **191**, 2362-2370.

62. T. J. Lawton, G. E. Kenney, J. D. Hurley and A. C. Rosenzweig, The CopC Family: Structural and Bioinformatic Insights into a Diverse Group of Periplasmic Copper Binding Proteins, *Biochemistry*, 2016, **55**, 2278-2290.

63. X. Morosov, C. F. Davoudi, M. Baumgart, M. Brocker and M. Bott, The copper-deprivation stimulon of *Corynebacterium glutamicum* comprises proteins for biogenesis of the actinobacterial cytochrome bc_1-aa_3 supercomplex, *J Biol Chem*, 2018, **293**, 15628-15640.

64. A. Durand, A. Azzouzi, M. L. Bourbon, A. S. Steunou, S. Liotenberg, A. Maeshima, C. Astier, M. Argentini, S. Saito and S. Ouchane, *c*-Type Cytochrome Assembly Is a Key Target of Copper Toxicity within the Bacterial Periplasm, *MBio*, 2015, **6**, e01007-01015.

65. A. Ziller and L. Fraissinet-Tachet, Metallothionein diversity and distribution in the tree of life: a multifunctional protein, *Metallomics*, 2018, **10**, 1549-1559.

66. D. Osman, K. J. Waldron, H. Denton, C. M. Taylor, A. J. Grant, P. Mastroeni, N. J. Robinson and J. S. Cavet, Copper homeostasis in *Salmonella* is atypical and copper-CueP is a major periplasmic metal complex, *J Biol Chem*, 2010, **285**, 25259-25268.

67. T. G. Gaule, M. A. Smith, K. M. Tych, P. Pirrat, C. H. Trinh, A. R. Pearson, P. F. Knowles and M. J. McPherson, Oxygen Activation Switch in the Copper Amine Oxidase of *Escherichia coli*, *Biochemistry*, 2018, **57**, 5301-5314.

68. C. Dennison, S. David and J. Lee, Bacterial copper storage proteins, *J Biol Chem*, 2018, **293**, 4616-4627.

69. E. Ladomersky and M. J. Petris, Copper tolerance and virulence in bacteria, *Metallomics*, 2015, **7**, 957-964.

70. C. Rademacher and B. Masepohl, Copper-responsive gene regulation in bacteria, *Microbiology*, 2012, **158**, 2451-2464.

71. S. Merchant and L. Bogorad, Regulation by copper of the expression of plastocyanin and cytochrome c_{552} in *Chlamydomonas reinhardi*, *Mol Cell Biol*, 1986, **6**, 462-469.

72. I. Rayment, G. Wesenberg, T. E. Meyer, M. A. Cusanovich and H. M. Holden, Three-dimensional structure of the high-potential iron-sulfur protein isolated from the purple phototrophic bacterium *Rhodocyclus tenuis* determined and refined at 1.5 A resolution, *J Mol Biol*, 1992, **228**, 672-686.

73. R. Overbeek, M. Fonstein, M. D'Souza, G. D. Pusch and N. Maltsev, The use of gene clusters to infer functional coupling, *Proc Natl Acad Sci U S A*, 1999, **96**, 2896-2901.

74. K. Marrero, A. Sanchez, L. J. Gonzalez, T. Ledon, A. Rodriguez-Ulloa, L. Castellanos-Serra, C. Perez and R. Fando, Periplasmic proteins encoded by VCA0261-0260 and VC2216 genes together with copA and cueR products are required for copper tolerance but not for virulence in *Vibrio cholerae*, *Microbiology*, 2012, **158**, 2005-2016.

75. S. Monchy, M. A. Benotmane, R. Wattiez, S. van Aelst, V. Auquier, B. Borremans, M. Mergeay, S. Taghavi, D. van der Lelie and T. Vallaeys, Transcriptomic and proteomic analyses of the pMOL30-encoded copper resistance in *Cupriavidus metallidurans* strain CH34, *Microbiology*, 2006, **152**, 1765-1776.

76. S. Monchy, M. A. Benotmane, P. Janssen, T. Vallaeys, S. Taghavi, D. van der Lelie and M. Mergeay, Plasmids pMOL28 and pMOL30 of *Cupriavidus metallidurans* are specialized in the maximal viable response to heavy metals, *J Bacteriol*, 2007, **189**, 7417-7425.

77. P. I. Trasnea, M. Utz, B. Khalfaoui-Hassani, S. Lagies, F. Daldal and H. G. Koch, Cooperation between two periplasmic copper chaperones is required for full activity of the cbb_3 -type cytochrome c oxidase and copper homeostasis in *Rhodobacter capsulatus*, *Mol Microbiol*, 2016, **100**, 345-361.

78. H. G. Koch, O. Hwang and F. Daldal, Isolation and characterization of *Rhodobacter capsulatus* mutants affected in cytochrome cbb_3 oxidase activity, *J Bacteriol*, 1998, **180**, 969-978.

79. H. G. Koch, C. Winterstein, A. S. Saribas, J. O. Alben and F. Daldal, Roles of the ccoGHIS gene products in the biogenesis of the cbb(3)-type cytochrome c oxidase, *J Mol Biol*, 2000, **297**, 49-65.

80. M. Utz, A. Andrei, M. Milanov, P. I. Trasnea, D. Marckmann, F. Daldal and H. G. Koch, The Cu chaperone CopZ is required for Cu homeostasis in *Rhodobacter capsulatus* and influences cytochrome cbb_3 oxidase assembly, *Mol Microbiol*, 2019, **111**, 764-783.

Table 1. Known or putative Cu-related proteins of *R. capsulatus*

RCAP_rcc Number[a]	Uniprot Entry	Protein (*gene*) name	Location[b]	Cu-Response[c]	Reference
Rcc00044[d]	**Q52720**	**Periplasm facing copper-binding protein SenC (*senC*)**	**CM**	nr	[29]
Rcc00088	D5AKL1	Uncharacterized metal-sensing transcriptional regulator CsoR (*csoR*)	C	nr	-
Rcc00612	D5ANM3	Periplasmic protein CusF (*cusF*)	P	nr	-
Rcc00613	D5ANM4	Transcriptional regulator, TetR family CusR (*cusR*)	C	nr	-
Rcc00614	D5ANM5	RND efflux system, CusC (*cusC*)	OM	nr	-
Rcc00615	D5ANM6	RND efflux system, CusB (*cusB*)	CM	nr	-
Rcc00616	D5ANM7	RND efflux system, CusA (*cusA*)	CM	nr	-
Rcc01157	**D5ARP4**	*cbb$_3$*-**type Cox subunit N (*ccoN*)**	**CM**	**R**	[78]
Rcc01158	**D5ARP5**	*cbb$_3$*-**type Cox subunit O (*ccoO*)**	**CM**	**R**	(73)
Rcc01159	**D5ARP6**	*cbb$_3$*-**type Cox subunit Q (*ccoQ*)**	**CM**	nr	(73)
Rcc01160	**D5ARP7**	*cbb$_3$*-**type Cox subunit P (*ccoP*)**	**CM**	**R**	(73)
Rcc01161	**D5ARP8**	*cbb$_3$*-**type Cox biogenesis, CcoG (*ccoG*)**	**CM**	**R**	[79]
Rcc01162	**D5ARP9**	*cbb$_3$*-**type Cox biogenesis, CcoH (*ccoH*)**	**CM**	nr	(74)
Rcc01163	**D5ARQ0**	*cbb$_3$*-**type Cox biogenesis, CcoI (*ccoI*)**	**CM**	nr	(74)
Rcc01164	**D5ARQ1**	*cbb$_3$*-**type Cox maturation, CcoS (*ccoS*)**	**CM**	nd	(74)
Rcc01844	D5AUF0	Sensor histidine kinase, CusS (*cusS*)	CM	nr	-
Rcc02109	**D5AV57**	**Uncharacterized protein next to *cutO***	**P**	**R**	[53]
Rcc02110	**D5AV58**	**Multicopper oxidase (MCO), CutO (*cutO*)**	**P**	**R**	(50)
Rcc02111	**D5AV59**	**Uncharacterized protein next to *cutO***	**P**	nd	(50)

Rcc02191	D5AKT1	Transcriptional regulator, MerR family CueR (*cueR*)	C	nr	-
Rcc02192	**D5AKT2**	**MFS-type copper importer CcoA (*ccoA*)**	**CM**	nr	[16]
Rcc02646	**D5AN86**	**Periplasmic copper-binding protein PccA (*pccA*)**	**P**	nr	[77]
Rcc02805	D5AP29	Polyphenol oxidase	C	nr	-
Rcc03124	D5AR43	Uncharacterized protein next to CopZ	C	nr	-
Rcc03125	**D5AR44**	**Cytoplasmic copper binding protein CopZ (*copZ*)**	**C**	nr	[80]
Rcc03126	D5AR45	Uncharacterized protein (CXC motif, similar to *Bacillus subtilis* YphP)	P	nd	-
Rcp00043	D5AVG6	Pseudoazurin	P	nr	-
Rcp00070	D5AVJ1	FAD:protein FMN transferase (Flavin transferase) NosX (*nosX*)	P	nd	-
Rcp00071	D5AVJ2	Nitrous oxide reductase accessory protein NosL (*nosL*)	P	nr	-
Rcp00072	D5AVJ3	Copper ABC transporter, permease protein NosY (*nosY*)	CM	nr	-
Rcp00073	D5AVJ4	Copper ABC transporter, ATP-binding protein NosF (*nosF*)	CM	**R**	-
Rcp00074	D5AVJ5	Nitrous oxide reductase maturation protein NosD (*nosD*)	P	nr	-
Rcp00075	D5AVJ6	Nitrous-oxide (N$_2$O) reductase NosZ (*nosZ*)	P	**R**	-
Rcp00076	D5AVJ7	Nitrous-oxide reductase expression regulator NosR (*nosR*)	C	**R**	-

[a]Rcc (chromosome) and Rcp (plasmid) numbers refer to the gene number on *R. capsulatus* genome for the corresponding protein;

[b]**CM**, cytoplasmic membrane; **C,** cytoplasm; **P**, periplasm; **OM**, outer membrane;

[c]Response to either Cu excess (+Cu) or Cu depletion (+BCS) conditions in current study (see Results); **R**, responsive; nr, not responsive; ND, not identified by MS under the conditions used;

[d]**bold** entries indicate the proteins that have been studied earlier, and regular fonts correspond to those that are recognized by high degree of homologies using protein BLAST (https://blast.ncbi.nlm.nih.gov/).

Table 2. *R. capsulatus* **proteins whose abundances are changed in +Cu or +BCS growth conditions**

(A) Cu-excess (+Cu)

RCAP rcc Number[a]	Uniprot Entry	p-value (t-test)	Fold-Change Up ((+Cu)/Ctrl) or Down (Ctrl/(+Cu))	Protein Description (*gene name*, homology)	Location[b]
Rcc02110	D5AV58	5.7E-13	↑ 263	Multicopper oxidase family protein	P
Rcc02109	D5AV57	9.7E-11	↑ 58	Uncharacterized protein (metal-binding protein)	P
Rcc00098	D5AKM1	1.5E-08	↑ 12	TonB-dependent hemin receptor (*hmuR*)	OM
Rcc01445	D5AT83	1.1E-06	↑ 5.3	TonB-dependent receptor	OM
Rcc01047 *	D5AR01	4.7E-08	↑ 4.6	Iron siderophore/cobalamin ABC transporter	P
Rcc00880	D5AQ58	1.4E-09	↑ 4.5	CHAP domain protein	P
Rcc00738	D5APD1	1.2E-03	↑ 2.5	Uncharacterized protein (DUF1989 domain-containing)	C
Rcc00533 *	D5AN09	7.9E-03	↑ 2.3	Uncharacterized protein (DUF1800 domain-containing)	C
Rcc02554	D5AMK8	1.3E-02	↑ 2.1	NmrA family transcription regulator	C
Rcc00426	D5AMQ2	2.2E-03	↑ 2.0	Uncharacterized protein (pyruvate oxidase)	C
Rcc00890 *	D5AQ68	2.8E-02	2.2 ↓	Uncharacterized protein (NosL family, TAT signal)	P
Rcc03281	D5ARY3	4.7E-03	2.2 ↓	Peroxiredoxin	C
Rcc03029 *	D5AQG4	2.4E-02	2.5 ↓	Uncharacterized protein (DUF4105 domain-containing)	CM
Rcc00722 *	D5APB5	6.5E-04	3.7 ↓	Lipoprotein, putative	P
Rcc02042	D5AV04	1.4E-02	4.3 ↓	Precorrin-6Y C5,15-methyltransferase (decarboxylating) (*cobL*)	C

(B) Cu-depleted (+BCS)

5

RCAP rcc Number[a]	Uniprot Entry	p-value (t-test)	Fold-Change Up ((+BCS)/Ctrl) or Down (Ctrl/(+BCS))	Protein Description (gene name)	Location[b]
Rcc00890 *	D5AQ68	2.0E-14	↑ 299	Uncharacterized protein (NosL family, TAT signal)	P
Rcc01028	D5AQY2	1.1E-14	↑ 24	Iron siderophore/cobalamin ABC transporter	P
Rcc00889	D5AQ67	4.2E-09	↑ 9.6	NosL family protein	P
Rcc03085	D5AQM0	3.1E-12	↑ 7.4	Cytochrome d ubiquinol oxidase, subunit I (cydA)	CM
Rcc00886	D5AQ64	6.1E-08	↑ 4.7	ABC transporter, ATP-binding protein	CM
Rcp00068	D5AVI9	6.9E-03	↑ 2.7	Peptidase, M4 family	CM
Rcc01747	D5AU53	5.5E-05	↑ 2.5	Cation/acetate symporter ActP-1 (actP1)	CM
Rcc00490	D5AMW6	6.1E-04	↑ 2.4	Methylenetetrahydrofolate reductase (metF)	C
Rcc00021	D5AKE4	3.8E-02	↑ 2.3	Cytochrome c peroxidase	P
Rcc03235	D5ARF4	2.6E-03	↑ 2.1	Monosacharide ABC transporter, permease protein	CM
Rcc00533 *	D5AN09	9.1E-03	↑ 2.1	Uncharacterized protein (DUF1800 domain-containing)	C
Rcc01766	D5AU72	1.8E-05	2.0 ↓	Chemotaxis protein (cheY3)	C
Rcc02627	D5AN67	1.1E-02	2.0 ↓	Penicillin-binding protein 4 (dacB)	P
Rcc02117	D5AV65	1.8E-06	2.0 ↓	Methyl-accepting chemotaxis protein	CM
Rcc00253	D5ALG2	7.0E-03	2.1 ↓	Major facilitator superfamily MFS_1	CM
Rcc03177	D5AR96	5.4E-05	2.1 ↓	EAL domain protein	CM
Rcc02617	D5AN57	8.9E-05	2.1 ↓	5'-nucleotidase (ushA)	P
Rcc01593	D5ATP9	2.7E-03	2.1 ↓	Phosphoadenylyl-sulfate reductase (thioredoxin) (cysH)	C
Rcc00504	D5AMY0	5.0E-06	2.2 ↓	ATPase, PP-loop family	CM
Rcc01849	D5AUF5	1.0E-03	2.2 ↓	Uncharacterized protein (PAS domain-containing)	C

5

Rcc01096	D5ARI5	4.4E-03	2.2 ↓	Aminobenzoyl-glutamate utilization protein B (abgB)	C
Rcc03176	D5AR95	1.7E-04	2.2 ↓	PAS/PAC sensor domain protein	CM
Rcc03029 *	D5AQG4	2.2E-02	2.2 ↓	Uncharacterized protein (DUF4105 domain-containing)	CM
Rcc01761	D5AU67	4.4E-03	2.2 ↓	Uncharacterized protein	C
Rcc01767	D5AU73	9.1E-04	2.2 ↓	CheX protein (cheX)	CM
Rcp00076	D5AVJ7	9.5E-03	2.2 ↓	Nitrous-oxide reductase expression regulator (nosR)	CM
Rcc03486	D5ASW9	5.7E-06	2.3 ↓	Chemotaxis protein MotA (motA)	CM
Rcc02069	D5AV31	5.8E-04	2.3 ↓	TPR repeat domain protein	C
Rcc01763	D5AU69	1.5E-04	2.3 ↓	Chemotaxis protein methyltransferase (cheR3)	C
Rcc01765	D5AU71	2.6E-07	2.4 ↓	Chemotaxis protein CheA-2 (cheA2)	C
Rcc02611	D5AN51	2.0E-04	2.4 ↓	Methyl-accepting chemotaxis protein McpA-3 (mcpA3)	CM
Rcc02832	D5AP56	7.3E-03	2.4 ↓	PTS system, IIA component	CM
Rcc01355	D5ASL0	1.7E-05	2.4 ↓	Methyl-accepting chemotaxis sensory transducer	CM
Rcc01764	D5AU70	8.7E-06	2.4 ↓	Chemotaxis protein CheW-2 (cheW2)	C
Rcc00184	D5AL93	1.0E-03	2.4 ↓	Outer membrane efflux protein	OM
Rcc01350	D5ASK5	8.7E-04	2.5 ↓	Uncharacterized protein (methyl-accepting chemotaxis)	C
Rcc03452	D5AST5	1.1E-02	2.5 ↓	Sensor histidine kinase protein	CM
Rcc01161	D5ARP8	2.9E-10	2.5 ↓	cbb_3-type Cox accessory protein CcoG (ccoG)	CM
Rcc00180	D5AL89	2.7E-04	2.6 ↓	Hpt domain protein	C
Rcc01758	D5AU64	3.0E-04	2.6 ↓	Methyl-accepting chemotaxis protein McpA-2 (mcpA2)	CM
Rcc01075	D5AR29	4.3E-04	2.6 ↓	Methyl-accepting chemotaxis protein	CM

Rcc01047 *	D5AR01	9.1E-03	2.7 ↓	Iron siderophore/cobalamin ABC transporter	P
Rcc00759	D5APF2	5.5E-03	2.7 ↓	Methyl-accepting chemotaxis protein McpB (*mcpB*)	CM
Rcc03323	D5AS25	5.3E-04	2.7 ↓	Anti-sigma factor antagonist (*rsbV*)	C
Rcc01139	D5ARM6	5.1E-05	2.8 ↓	Uncharacterized protein	C
Rcc00722 *	D5APB5	1.1E-02	2.9 ↓	Lipoprotein, putative	P
Rcc03014	D5AQF2	3.2E-04	2.9 ↓	Methyl-accepting chemotaxis sensory transducer	CM
Rcc03324	D5AS26	1.0E-02	2.9 ↓	Anti-sigma regulatory factor (*rsbW*)	C
Rcc00007	D5AUZ3	2.2E-11	2.9 ↓	Flagellar hook protein FlgE (*flgE*)	E
Rcc01667	D5ATX3	1.4E-03	3.0 ↓	Methyl-accepting chemotaxis sensory transducer	OM
Rcc03067	D5AQK2	2.2E-07	3.0 ↓	Uncharacterized protein (*EfeM* lipoprotein)	P
Rcc00760	D5APF3	8.0E-05	3.2 ↓	Methyl-accepting chemotaxis protein McpA-1 (*mcpA1*)	CM
Rcc01726	D5AU32	6.8E-05	3.2 ↓	Methyl-accepting chemotaxis protein McpH (*mcpH*)	CM
Rcc01353	D5ASK8	2.9E-04	3.3 ↓	Chemotaxis protein CheA-1 (*cheA1*)	C
Rcc00644	D5ANQ5	2.1E-04	3.3 ↓	Methyl-accepting chemotaxis protein McpX (*mcpX*)	CM
Rcp00073	D5AVJ4	4.8E-08	3.6 ↓	Copper ABC transporter, ATP-binding protein (*nosF*)	CM
Rcc00747	D5APE0	4.5E-05	3.6 ↓	Uncharacterized protein (Phasin, PhaP)	P
Rcc01423	D5AT61	3.0E-03	3.7 ↓	Uncharacterized protein	C
Rcc00620	D5ANN1	1.7E-05	4.2 ↓	Response regulator receiver modulated diguanylate cyclase/phosphodiesterase	CM
Rcc02610	D5AN50	1.9E-07	4.2 ↓	Uncharacterized protein	P
Rcc01157	D5ARP4	7.2E-05	4.2 ↓	cbb$_3$-type Cox subunit I (*ccoN*)	CM
Rcc00142	D5AKR5	4.8E-06	5.6 ↓	Uncharacterized protein	C
Rcc01158	D5ARP5	1.5E-09	5.6 ↓	cbb$_3$-type Cox subunit II or CcoO (*ccoO*)	CM
Rcc01160	D5ARP7	3.6E-11	7.1 ↓	cbb$_3$-type Cox subunit III or CcoP (*ccoP*)	CM

Rcp00075	D5AVJ6	5.6E-17	20.0 ↓	Nitrous-oxide (N$_2$O) reductase (*nosZ*)	P

[a]Proteins that showed significant abundance changes under (**A**) Cu excess (+Cu) or (**B**) Cu depletion (+BCS) conditions with p-

Gene or strain	Known or putative protein	Mutation	[a]Ps growth			[a]Res growth			[a]Nadi	
Controls			CTRL	+Cu	+BCS	CTRL	+Cu	+BCS	CTRL	+Cu
[b]MT1131	wild type	n/a	+	+	+	+	+	+	+	+
[b]SE8 (*Δrcc02192*)	CcoA	*ccoA::spe*	+	+	+	+	+	+	-	+
[b]SE15 (*Δrcc02110*)	CutO	*cutO::kan*	+	-	+	+	+	+/-	+	+
[b]SE25 (*Δrcc01180*)	CopA	*copA::kan*	+	+/-	+	+	-	+	+	+
Mutants										
[c]Δ *[rcc00094-00098]*	Hemin transport [d](+Cu, up)	[e]*in frame-del*	+	+	+	+	+	+	+	+
Δ *[rcc00885-00891]*	ABC transporter (+BCS, up)	*del::gen*	+	+	+	+	+	+	+	+

value< 0.05 and up- or down -fold-change greater than 2.0; Rcc (chromosome) and Rcp (plasmid) numbers refer to the gene number on the *R. capsulatus* genome for the corresponding protein;

[b]Localization deduced from PSORTb, Uniprot and GO annotations, TMH predictors, SignalP and Pred-Tat;

C: cytoplasmic, P: periplasmic, CM: cytoplasmic membrane, OM: outer membrane, E: extracellular;

*Proteins that were significantly changed in both Cu excess and Cu depletion conditions.

Δrcc00738	Uncharacterized (+Cu, up)	*del::gen*	+	+	+	+	+	-	+	+
Δrcc01445	TonB-dependent receptor (+Cu, up)	*del::gen*	+	+	+	+	+	-	+	+
Δ [rcc01027-01031]	Fe-siderophore ABC transporter (+BCS, up)	*del::gen*	+	+	+	+	+	+/-	+	+
Δ [rcc03065-03067]	Ferrous Fe uptake (+BCS, down)	*del::gen*	+	+	+	-	-	-	na	na
Δrcc01423	Uncharacterized (+BCS, down)	*in frame-del*	+	+	+	+	+/-	+/-	+	+
Δrcc02109	Uncharacterized (+Cu, up)	*del::gen*	+	-	+	+	+	+/-	+	+
Δrcc02111	Uncharacterized *	*del::gen*	+	-	+	+	+	+/-	+	+

Table 3. Phenotypic properties of *R. capsulatus* mutant lacking the selected Cu-responsive genes or gene clusters

[a]Growth was on Cu-sufficient (CTRL), Cu-excess (+Cu) and Cu-depleted (+BCS) minimal MedA, under photosynthetic (Ps) or respiratory (Res) growth conditions, and Nadi staining was performed using Res grown colonies, as described in Experimental Procedures. (+) and (-) refer to normal growth, and no growth, respectively; (+/-) refers to slow growth;

[b]MT1131, SE8, SE15 and SE25 strains were reported earlier [16, 17], and used here as control strains;

[c]The genes between the indicated numbers were deleted;

[d]up and down refer to the differential responses of the corresponding proteins to (+Cu) or (+BCS) as compared to Cu-sufficient growth conditions;

[e]*in frame-del* and *del::spe* or *::kan* or *::gen* indicate the type of the mutations constructed (Experimental Procedures).

*The protein Rcc02111 was not identified in the current study, but is located next to *cutO* (*rcc02110*) corresponding to CutO/MCO (multicopper oxidase) [53].

1
2
3
4
5
6
7
8
9
10
11
12
13
14
15
16
17
18
19
20
21
22
23
24
25
26
27
28
29
30
31
32
33
34
35
36
37
38
39
40
41
42
43
44
45
46
47

5
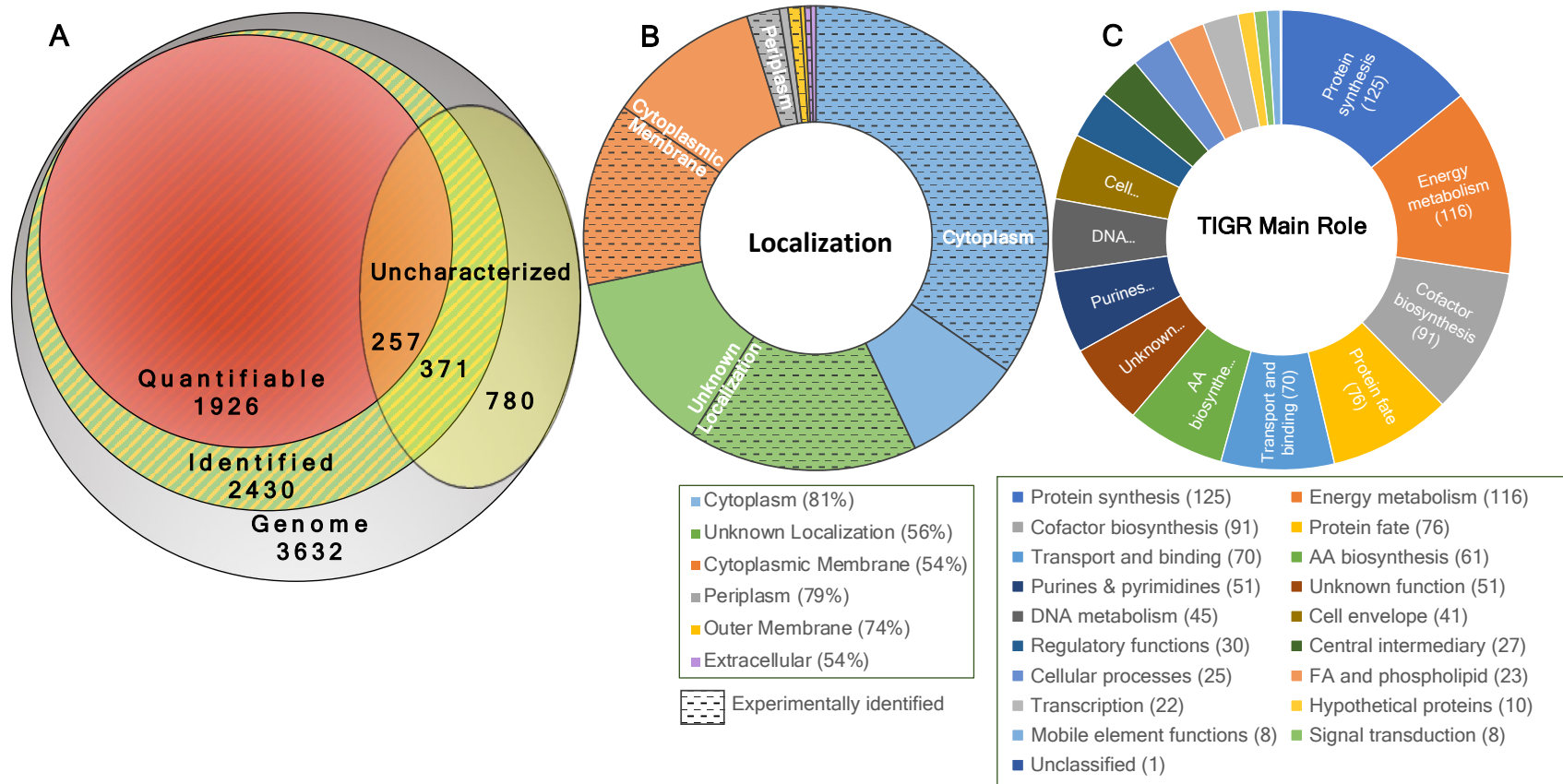
Figure 1. *Rhodobacter capsulatus* **proteome. (A)** Venn diagram showing experimentally identified proteins among those encoded by the *R. capsulatus* genome, and among the identified proteins, those that are quantified as described in the Experimental Procedures. The total number of uncharacterized proteins and their distributions among the identified and the quantified proteins subcategories are indicated. **(B)** Distribution of *R. capsulatus* genome proteins among the various

6

cellular locations, with the experimentally identified proteins indicated by the shaded areas. Percentages refer to those identified by MS in this study. Localization information was obtained from PsortB (version 3.0.2; www.psort.org). **(C)** TIGR main role categories for the identified proteins with the assigned TIGRFAM annotations (www.tigrfams.jcvi.org release 15.0, 2014), extracted from UniprotKB. The top main roles are shown, with the number of proteins indicated for each category. Only 881 proteins, covering 36% of the identified proteins could be categorized using the TIGRFAM annotations.
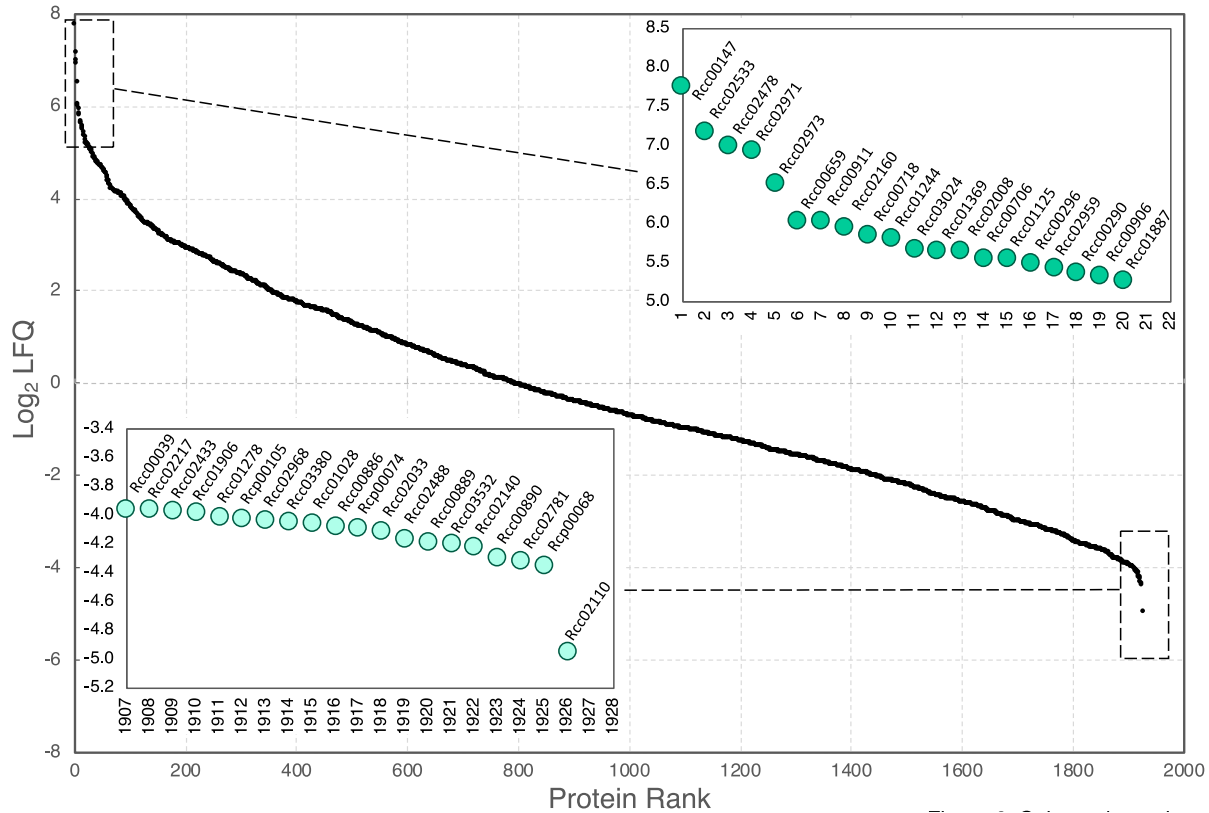
Figure 2. LFQ rank profile of quantified proteins for Cu-sufficient (control) samples.

The log$_2$(LFQ) intensity (mean of biological and technical repeats) was plotted against the

protein rank based on the LFQ values, showing the distribution of the 1926 quantified

proteins in the Cu-sufficient (control) samples. Note that log$_2$(LFQ) spans from ~ -5.3 to +

7.7, corresponding to about 8000-fold variation. The insets on the upper right and lower

left corners show the identities of the 20 highest- and 20 lowest-LFQ proteins.

The top 20 proteins: Rcc00147, Elongation factor Tu *tuf1*; Rcc02533, Light-harvesting

protein B-800/850, gamma chain *pucDE*; Rcc02478, 60 kDa chaperonin *groL*; Rcc02971,

ATP synthase subunit beta *atpD*; Rcc02973, ATP synthase subunit alpha *atpA*; Rcc00659,

Photosynthetic reaction center, H subunit *puhA*; Rcc00911, Propionyl-CoA carboxylase,

alpha subunit *pccA*; Rcc02160, Glyceraldehyde-3-phosphate dehydrogenase *gap3*; Rcc00718, Malate dehydrogenase *mdh*; Rcc01244, Polyamine ABC transporter *potD1*; Rcc03024, TRAP dicar- boxylate transporter *dctP3*; Rcc01369, ABC transporter, P substrate-binding protein; Rcc02008, Trigger factor *tig*; Rcc00706: Oligopeptide ABC transporter *oppA1*; Rcc01125: 30S ribosomal protein S1 *rpsA*; Rcc00296, Elongation factor G *fusA1*; Rcc02959, Polyamine ABC transporter *potD5*; Rcc00290. 50S ribosomal protein L7/L12 *rplL*; Rcc00906, Propionyl-CoA carboxylase *pccB*; Rcc01887, Isocitrate dehydrogenase [NADP] *icd.*

The bottom 20 proteins: Rcc00039, Nucleotidyltransferase family protein; Rcc02217, Glycosyl transferase, group 1; Rcc02433, Uncharacterized protein; Rcc01906, Uncharacterized protein; Rcc01278, Conserved domain protein; Rcp00105, Transcriptional regulator, XRE family; Rcc02968, Uncharacterized protein; Rcc03380, SsrA-binding protein (Small protein B;*smpB)*; Rcc01028, Iron siderophore/cobalamin ABC transporter; Rcc00886, ABC transporter, ATP-binding protein; Rcp00074, Nitrous oxide maturation protein *nosD*; Rcc02033, Precorrin 3B synthase *cobZ*; Rcc02488, Uncharacterized protein; Rcc00889, NosL family protein; Rcc03532, Formamidopyrimidine-DNA glycosylase *mutM*; Rcc02140, Extracellular ligand-binding receptor; Rcc00890, Uncharacterized protein; Rcc02781, FAD dependent oxidoreductase; Rcp00068, Peptidase, M4 family; Rcc02110, Multicopper oxidase family protein.
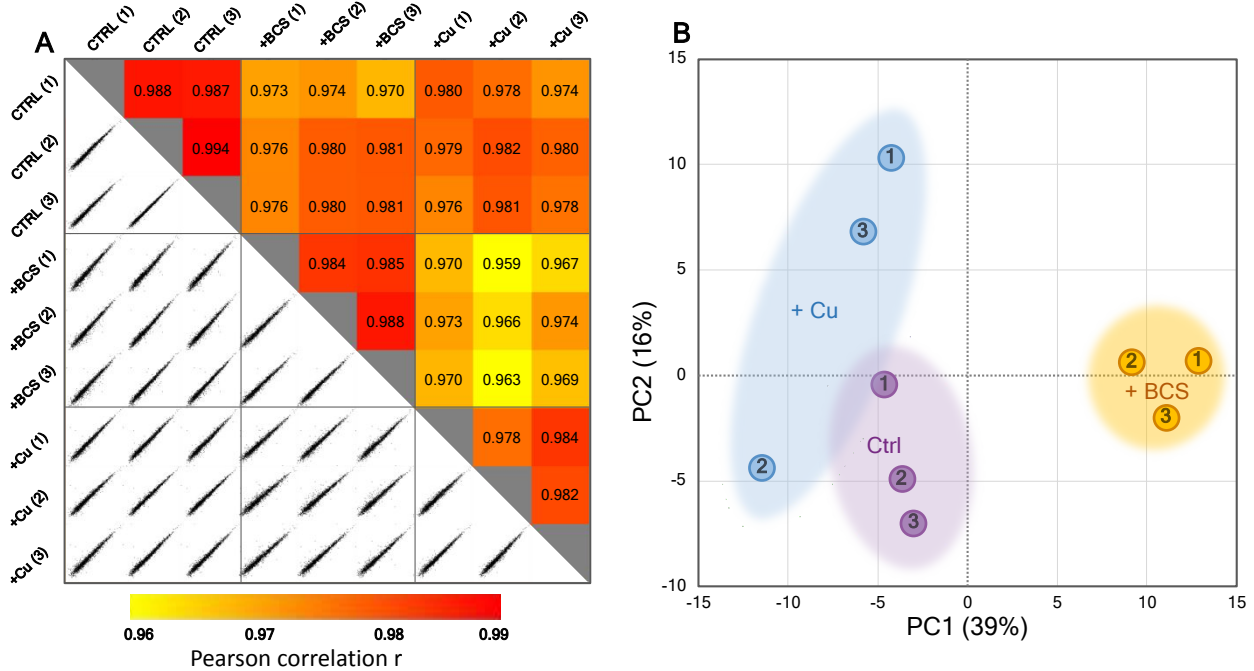
Figure 3. Proteomic data quality for *R. capsulatus* cells grown under various Cu concentrations. (A) Color-coded Pearson correlations and multi-scatter LFQ plots depicting the three biological replicates (1-3) and the three Cu (+BCS, +Cu, Ctrl (Cu-sufficient)) concentrations used. Only the reliably quantified 1926 proteins are included, with each biological replicate representing mean LFQ values of the technical repeats. The correlations observed are uniformly high (> 0.959) throughout all conditions, and are highest (0.978 to 0.994) among the biological replicates for a fixed Cu level, and lowest (0.959 to 0.974) between the two extreme Cu levels, +BCS and +Cu. **(B)** Principle component analysis (PCA) of the LFQ based protein expression values. Note that the biological replicates (1-3) group together within each Cu growth condition, and the largest separation corresponds to the two extreme Cu concentrations, +Cu and +BCS.

6

Technical repeats were averaged, and 1797 of the 1926 proteins with non-zero LFQ values were used for the PCA analysis. Both the Pearson correlation and PCA analyses were performed prior to missing data imputation (Perseus, www.coxdocs.org).
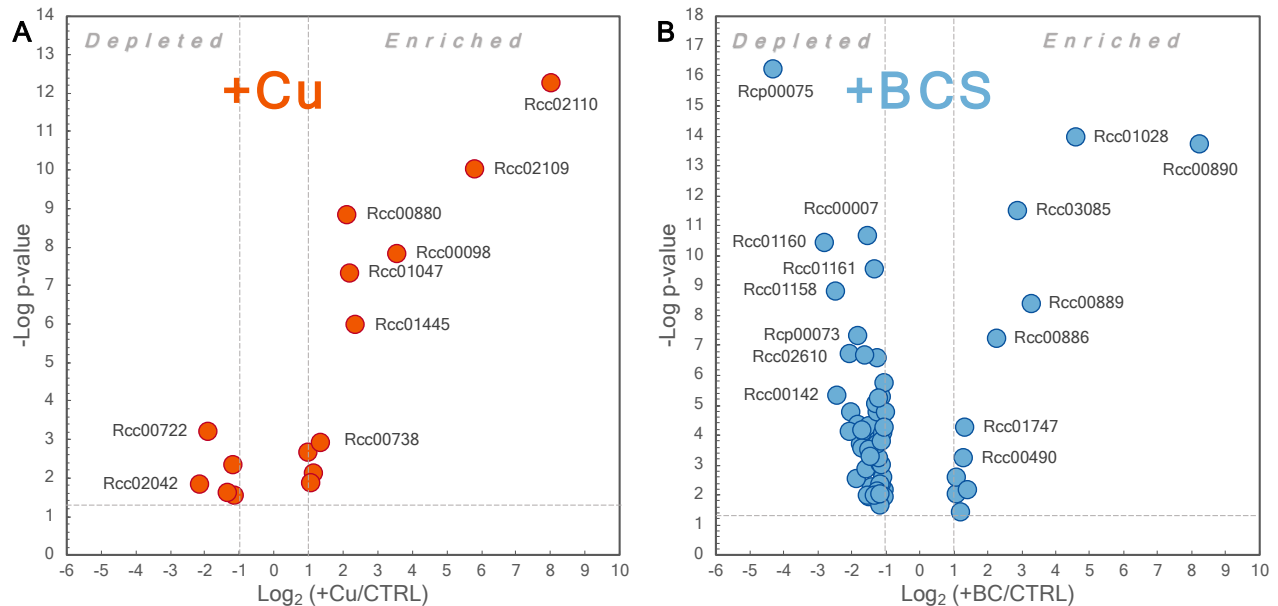
Figure 4. Volcano plots showing quantitative enrichment or depletion of *R. capsulatus* proteins by Cu availability. The t-test -log p value *versus* $\log_2$ fold change for Cu supplementation (+Cu/Ctrl) **(A)** and Cu depletion (+BCS/Ctrl) **(B)** as compared to Cu-sufficient control (Ctrl) conditions. The vertical and horizontal dashed lines indicate the 2 fold-changes and the p value of 0.05, respectively. The differentially affected proteins that satisfy both of these significance cutoff criteria (p value <0.05 and fold-change >2) are indicated in red and blue circles for + Cu and +BCS, respectively.
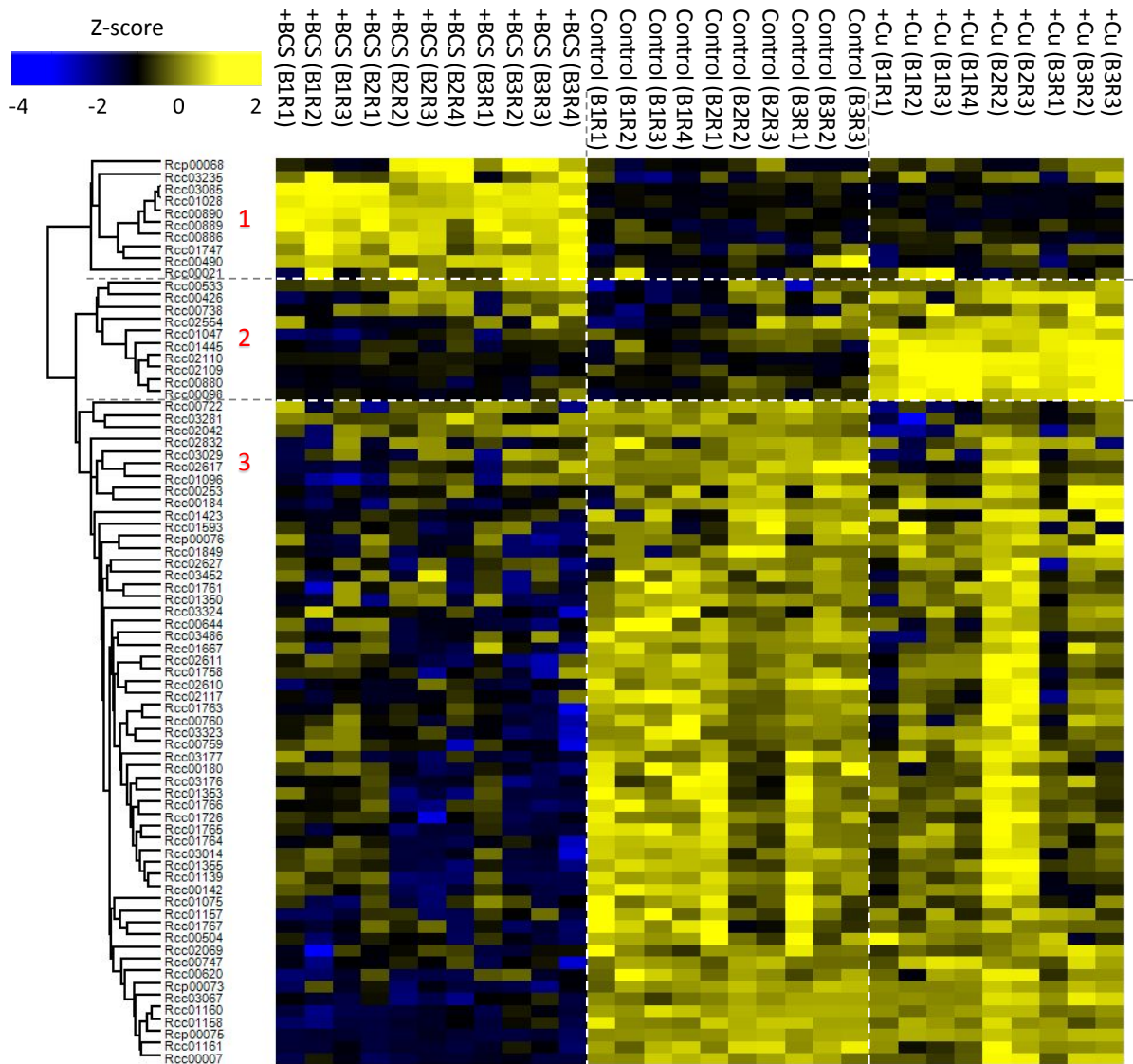
Figure 5. Hierarchical clustering of significantly changed proteins. A heat map of z-scored $\log_2$ LFQ intensities of the 75 Cu-responsive proteins with differential abundance changes in response to different Cu amounts was generated using unsupervised Euclidean hierarchical clustering (Perseus, www.coxdocs.org). The samples are identified by Cu condition (Ctrl, +Cu and +BCS), biological repeat (B1, B2, B3) and technical repeat (R1, R2, R3, R4). The proteins segregated into three main clusters,

6

indicated as 1, 2 and 3 on the dendrogram (left), separated by dotted lines and shown by

the differentiated blue-yellow color groups in the heat map.
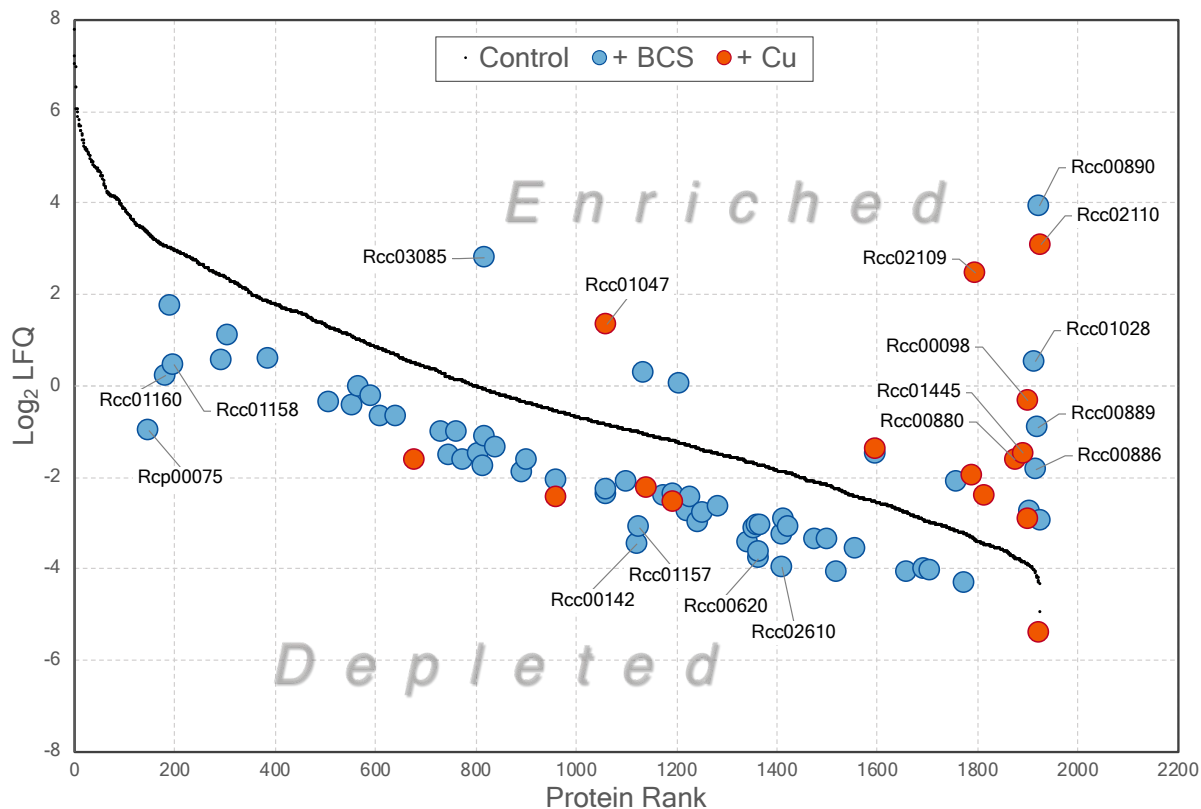
Figure 6. LFQ abundance of overproduced and underproduced proteins relative to the control (Cu-sufficient) in cells exposed to different concentrations of Cu. The mean LFQ values of the 75 differentially regulated proteins, under +Cu or +BCS conditions, were compared to their counterparts in Cu-sufficient control cells in the protein LFQ rank plot of Figure 2. Black dots represent $\log_2$ LFQ in Ctrl (Cu-sufficient) conditions; red and blue circles represent the LFQ for selected proteins in Cu-excess (+Cu), and Cu-depleted (+BCS) conditions, respectively. Proteins that are highly overproduced or underproduced (p-value <0.01, fold-change >4) are labeled. Note that the LFQ value of a

given protein does not necessarily indicate its cellular amount, and only used here for

differential comparison purposes.
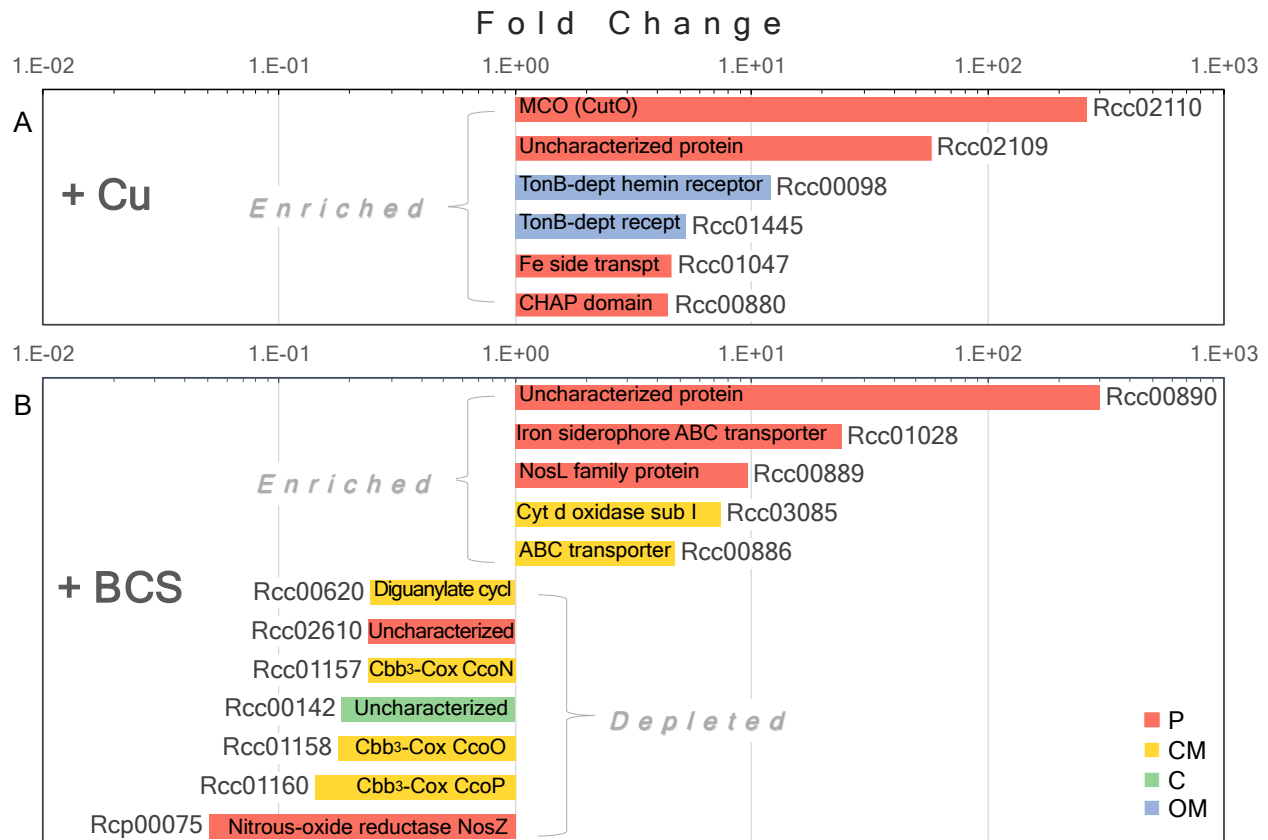
Figure 7. Fold-changes of strongly Cu-responsive *R. capsulatus* proteins. The fold-

changes of the 18 most highly Cu-responsive (p-value <0.01 and fold-change >4) proteins

that are overproduced or underproduced in cells grown under (**A**) Cu-excess (+Cu/Ctrl),

and **(B)** Cu-depletion (+BCS/Ctrl) conditions. Cellular localizations of these proteins are

color-coded as indicated.

6
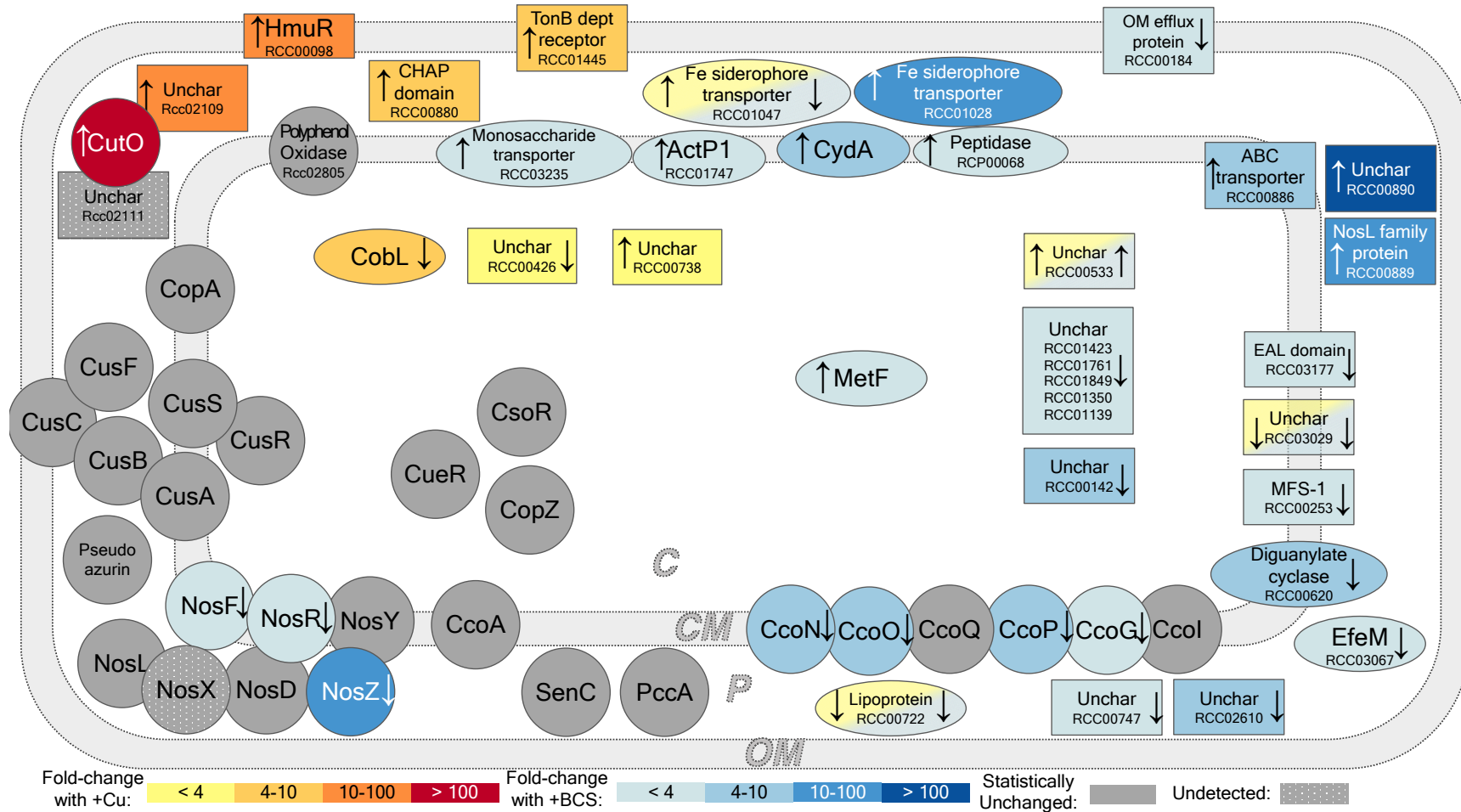
Figure 8. Cellular distribution of Cu-related proteins in the presence or absence of Cu in the growth medium. Proteins of unchanged abundance are shown in gray, and those that are predicted but not identified in this study are in dotted gray. Proteins that exhibited differential abundance changes in +Cu and +BCS growth conditions are colored using different

6

shades of red-yellow and blue, respectively, based on the exhibited fold changes with respect to Cu-sufficient (control) cells. For each protein, up or down arrows refer to its overproduction or underproduction, respectively, in response to +Cu or +BCS. The *R. capsulatus* proteins that are known, or predicted (based on homology) to be involved in Cu homeostasis are indicated as circles, those that have attributed functions as ellipsoids, and those that are uncharacterized (including family members) as rectangles. Proteins that are functionally related to each other, such as enzyme subunits or assembly factors, are grouped near to each other. Of the Cu-responsive proteins listed in **Table 2**, those that are related to chemotaxis or motility are not included in the figure.

1
2
3
4
5
6
7
8
9
10
11
12
13
14
15
16
17
18
19
20
21
22
23
24
25
26
27
28
29
30
31
32
33
34
35
36
37
38
39
40
41
42
43
44
45
46
47
48
49
50
51
52
53
54
55
56
57
58
59
60

7